CALT-68-573
ERDA RESEARCH
AND DEVELOPMENT
REPORT

Phenomenology of High p_T Scattering*

G. C. FOX†

California Institute of Technology, Pasadena, California, 91125

ABSTRACT

Constituent scattering models are critically compared to correlation data at high p_T. A simple quark quark scattering model is generally successful although some features of the new data suggest it may not be the complete picture.

Invited talk at Brookhaven APS meeting, October 1976.

†Supported in part by the Alfred P. Sloan Foundation.
*Work supported in part by the U. S. Energy Research Development and Administration under Contract No. E(11-1)-68.

I. Introduction and the Models

There have been many excellent experimental[1-5] and theoretical[6-10] reviews of high p_T scattering. In this talk we will not try to be complete but rather consider how some of the correlation measurements can be quantitatively used to distinguish competing models. We will give a short account of the lessons of the single particle measurements in Section III but for a proper treatment the reader is referred to both the pioneering theory (phenomenology) papers[11-16] and the reviews already mentioned. The experimental observation that the single particle distribution at high p_T takes the form

$$E\, d^3\sigma/d^3p \propto p_T^{-N} f(x_T, \theta_{cm}) \qquad (1)$$
$$x_T = 2p_T/\sqrt{s}$$

argues persuasively[6] for a constituent picture typified below:

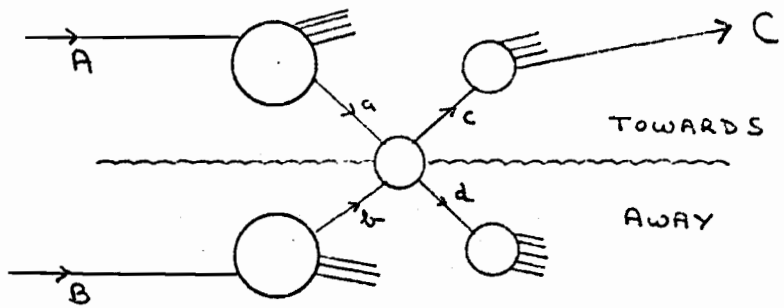

Here the constituents a,b of hadrons A,B undergo a large angle scattering to become c,d respectively. The observed trigger particle C is formed by the fragmentation of the constituent c. Such a picture for high p_T scattering leads to several correlation predictions of which perhaps the most distinctive is the approximate collinearity of A, B, C and d seen through its decay products. These

expectations were reviewed by Frisch[1] and seem to be supported by the current data. Such comparisons justify my decision only to consider constituent scattering models in this paper. However as mentioned above, I have not tried to collect together all the evidence for a constituent picture but will rather assume this general approach and ask if the data gives us any way of distinguishing the different constituent models. These models differ from one another both in the choice of constituents and the form of the hard scattering amplitude ab → cd. We define the two basic models below:

(i) Model Q: a,b,c and d are all quarks:

This idea was initially abandoned, as taking the natural choice of scale invariant vector gluon exchange for the qq → qq scattering amplitude, one finds a p_T^{-4} not a p_T^{-8} behavior for the high p_T pion production cross-section. However Field and Feynman[16] (FF) take the point of view that quark-quark scattering is responsible for large p_T hadron production but that $d\sigma/d\hat{t}$ is not known theoretically and must be taken from experiment. The form

$$d\sigma/d\hat{t} \propto 1/(-\hat{s}\,\hat{t}^3) \qquad (2)$$

was chosen as leading to the correct p_T and θ_{cm} dependence in (1). As described in Section III, this model naturally gets the correct x_T dependence. The invariants $\hat{s}$, $\hat{t}$ in (2) refer to the qq → qq amplitude and are illustrated in Fig. 1. Correlations in this model will be discussed in Ref. 17 and earlier work with related models can be found in Refs. 18 to 20.

(ii) Model C: Constituent Interchange Model (CIM):

In the constituent interchange model C[6,14], quark particle scattering is supposed to dominate. For instance for π^+ production, a typical diagram is the ($\bar{d}$) exchange

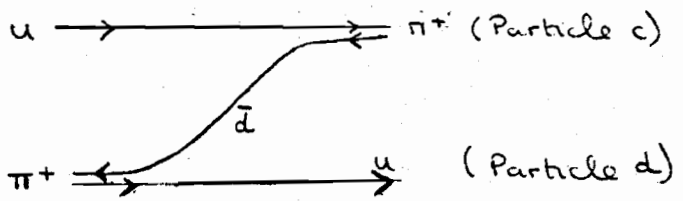

The CIM model naturally gives the correct p_T and x_T dependence in (1) at $\theta_{cm} = 90°$, and this parameter free prediction is very impressive. The θ_{cm} dependence of the model has not been tested in the literature. Ringland and Raitio have looked at correlation predictions in the CIM[21].

In Section III we review this success and show that the quark model Q (with maybe a simple generalization) can equally well describe the single particle data. Before then in Section II, we present the theoretical formalism and point out its critical features. We also discuss possible extensions (ambiguities) in our basic models Q and C. Note that the basic models Q and C are appealing because they have essentially no free parameters. We only present explicit calculations for them and not the extended models of Section II. The latter are introduced to give a framework for understanding failures of our basic models. The different models are summarized in Table 6 which will be found in the concluding section.

After this we turn to the correlation data where we have the kinematics illustrated in figure 2 and already used by Frisch[1]. This figure defines[22] θ, ϕ, p_x, x_e and p_{out}. In Section IV, we consider new jet trigger data and show that it greatly favors the quark constituent model Q. In Section V we show that model Q also agrees very well with the "towards" (i.e. trigger side - see figures 1 and 2) correlation data. These two sections together support

rather strongly the notion that the observed high p_T single mesons are fragments of quarks. Unfortunately although quark fragmentation is a simple way of describing the data, one can perhaps reproduce it with complicated (and as yet undefined) versions of the CIM model. For baryon trigger particles or in any case on the other ("away" i.e. fragmentation of d) side, the situation is less clear. In Section VI we show that the seemingly innocent charged particle associated multiplicity measurements place severe constraints on the models. Proton production is especially hard to understand in the Q model. In Section VII we look at rapidity shapes and in Section VIII x_e distributions of away side particles. No model does really well but there is no critical disagreement for either quark quark or CIM models except for the trigger p_T dependence of the away side x_e dependence. In fact if the current data on this is confirmed, it will be difficult to find any simple model to fit the observations. This and other conclusions will be found in the final section.

II. The Formalism

The general formalism for constituent scattering is nicely described in Ref. 6 and the single particle invariant cross-section is given by

$$E\, d^3\sigma/d^3p = \int d^2k_{Ta}\, d^2k_{Tb}\, d^2k_{TC}\, dx_a\, dx_b \qquad (3)$$

$$P_{a/A}(x_a,k_{Ta})\, P_{b/B}(x_b,k_{Tb})\, P_{C/c}(x_C,k_{TC})\, \frac{1}{\pi x_C}\, d\sigma/d\hat{t}(ab \to cd)$$

and illustrated below:

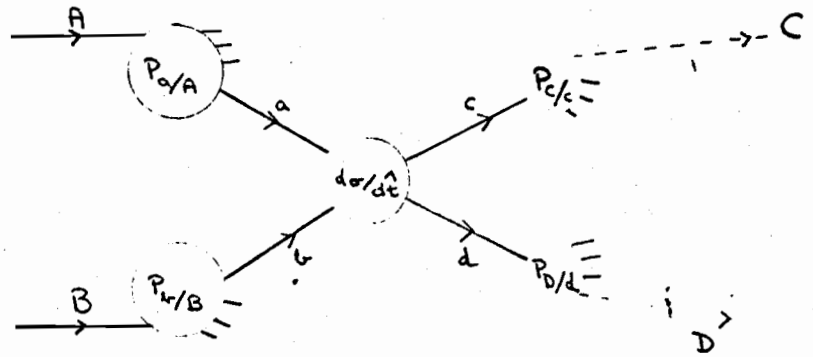

$P_{\beta/\alpha}$

Each of the probability functions $P_{\alpha/\beta}$ is a function of the longitudinal momentum fraction x_β and the transverse momentum $k_{T\beta}$ of β in α. (We use k_T to denote internal transverse momenta of constituents and p_T for observed hadronic transverse momenta.) In the CIM model we have $P_{C/c}(x_C,k_{TC}) \propto \delta(x_C - 1)$. As described by FF[16], the quark probabilities, either $P_{q/p}$ (quarks in hadrons) or $P_{\pi/q}$ (hadrons in quarks) are reasonably well determined by a careful analysis of lepton processes. Figure 3 compares their parameterization of $P_{\pi,K/q}$ with a variety of different lepton data: the consistency of the different determinations is very impressive. We will use the FF parameterizations in the following without further comment except to warn that the current determinations are only accurate to 20%. This much flexibility is implicit in any future theoretical curves. For the CIM model we also need $P_{\pi/p}$ which we will take to be proportional to the simple counting law[23] prediction $(1 - x_\pi)^5$.

Above we only discussed the x dependence but the transverse momentum dependence is also significant. This follows from a subtle trigger bias effect[24] illustrated below and in Fig. 4. In (2) the scattering cross-section $d\sigma/d\hat{t}$ falls

rapidly with p_T of c with respect to a. For a fixed trigger p_T of hadron C, $d\sigma/d\hat{t}$ thus enhances configurations where internal transverse momenta $k_{Ta,b}$ points towards C. As shown below, this effect decreases transverse momentum on the away side. Thus (a), (b) below have same trigger side p_{Tc} but (a) is enhanced by the above mechanism.

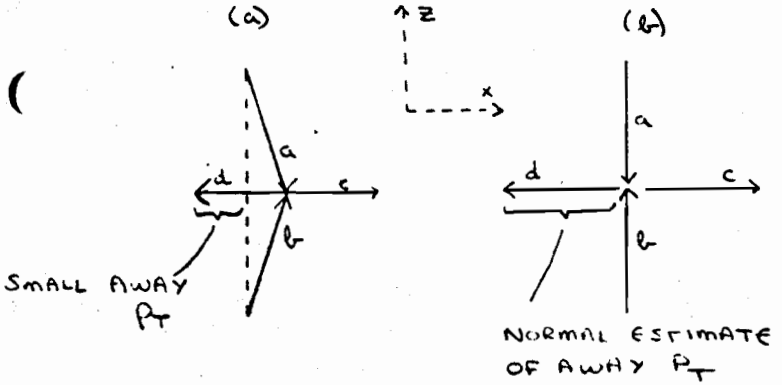

In the following we will assume that all transverse momenta dependence is like that observed in hadron reaction i.e. $\exp(-6k_T)$. This is supported for hadrons from quarks $P_{C/c}$, $P_{D/d}$ by SPEAR data: for quarks in hadrons ($P_{a/A}$, $P_{b/B}$), the μ pair data discussed by Lederman[25] at this conference suggests a larger mean p_T. Some of this experimental evidence is shown in Fig. 5 but we will defer a detailed discussion to a later paper[17]. We will however point out in Section VIII when our results are particularly sensitive to the mean k_T of quarks in hadrons. The simple choice $\exp(-6k_T)$ typically increases single particle cross-sections by a factor 2 and decreases away side distritutions by a somewhat smaller factor.

Enough of this subtlety; returning to Eq. (3) we note that in model Q the mean value of x_C is determined by a competition between two terms. $P_{C/c}$ (x_C) decreases with increasing x_C (cf. Fig. 3) while $d\sigma/d\hat{t}$ (as $p_{Tc} \sim$ the fixed p_{TC}/x_C)

does the opposite. The result is a mean x_C of .8 to .9 for the data to be discussed in this paper: the larger x_C corresponds to configurations ($\theta_{cm} = 20°$ or lower energies) where $d\sigma/d\hat{t}$ decreases faster with p_{Tc}. Further only values of $x_C \geq .6$ matter; $P_{C/c}$ (x_C) for $x_C \leq .6$ has little effect on the cross-section. Of course on the away side ($P_{D/d}$), this bias is not present and one is sensitive to the full range of x_D. Note that earlier work on quark quark scattering had estimated[8,10] a lower x_C: the higher value of FF leads to much better agreement with the towards correlation data than before.

Let us finish this section by discussing possible generalizations of our basic models Q and C introduced in Section I. If the proton had constituents (e.g. gluons) which had a smaller probability than quarks of giving hadrons at high $x_{C,D}$, then these new constituents would not affect the trigger side (as this is only sensitive to high x_C) but would substantially change the away side distributions. We will define model Q* as the extension to Q that allows additional constituents - in Sections III and VI we will mention diquarks and in Section VIII gluons. Earlier work[8] by Ellis, Jacob and Landshoff has discussed a model which essentially mixes Q with a CIM-like delta function $\delta(x_C-1)$ component. This we will call model D: the delta function raises the mean vlaue of x_C for single particle triggers. Although the model D cannot be ruled out, much of its motivation has now gone as the FF model Q automatically gets a higher mean x_C than the original quark quark component of Ref. 8.

Finally we should extend the simple CIM model to not only produce single particles but also resonances that decay into the observed trigger particle. We call this extension C^*; the correlation data clearly favors C^* over C. It is by no means clear that one can formulate C^* to both agree with the correlation data and retain the beautiful predictions of C for the single particle cross-sections. All these different models are summarized in Table 6 in the conclusions.

III. Single Particle Cross-Sections

As Brodsky and Gunion[10] have emphasized, the x_T and p_T dependence of the invariant cross-sections for the different particle types is in excellent agreement with the CIM model. Their results are reproduced in Table 1 which compares them with those of quark quark scattering. We have used the counting rules of Brodsky and Farrar[23] to derive the x_T and p_T dependencies. Model Q only has a problem with proton production. Maybe the data can be fit with a combination of qq → qq with subsequent quark → proton decay plus the "leading particle" term qp → qp; the latter is seemingly needed to explain the high $x_{\parallel}$ (triple Regge region) data of the CHLM collaboration[26]. However a single quark-diquark scattering term gives a much more natural explanation of the data. One would argue that diquarks are enhanced for proton production as (qq) prefers to decay at high x_C to protons rather than mesons. As shown in VI the correlation data can help choose the correct mechanism.

The CIM model has its own little problem. Thus the correlation data strongly suggests the generalized model C^* in which resonances M^* are produced and decay into the observed single particle. If

$$P_{\pi/M^*}(x_C) \sim (1 - x_C)^n \quad ,$$

then one must multiply all the naive CIM predictions by $(1 - x_T)^{n+1}$ - unfortunately the data already agrees with the naive $(1 - x_T)$ power laws without the extra $(1 - x_T)^{n+1}$. One cannot take n too small (e.g. n = -1 would restore single particle happiness) and still expect the C^* model to rescue the bad correlation predictions of the basic model. However maybe we haven't reached the region where the $(1 - x_T)$ fits are precise. For instance the naive power counting in Table 1 suggests disagreement between model Q and $\pi^- p \to \pi^o$ data[27] [$(1 - x_T)^3$ v. $(1 - x_T)^{1.6}$]; figure 6 shows theory and experiment actually agree very well.

Table 1

	Hard Scattering Process		90° Cross-Section * $pp \to \pi^o$ Production Cross-Section		
Observed Reaction	Quark Quark Scattering	CIM	qq Scattering	CIM[a]	Data[g]
$pp \to \pi^o, \pi^+$	qq→qq q→π	qM*→qM* M*→π	(c)	(b)	(b)
$pp \to \pi^-$	qq→qq q→π^-	qM*→qM* M*→π^-	$(1-x_T)$	(?)	$(1-x_T)^{.9}$
$pp \to \eta$	qq→qq q→η	qM*→qM* M*→η	~.5	const	~.5
$pp \to K^+$	qq→qq q→K^+	qM*→qM* M*→K^+	const	const	~.5
$pp \to K^-$	qq→qq (s,ū) quark →K (d)	qM*→qM* M*→K^-	$(1-x_T)^4$	$(1-x_T)^4$	$(1-x_T)^{2.9}$
	u quark →K^-	$q\bar{q}\to K^+K^-$	$(1-x_T)^2$	$(1-x_T)^2$	
$pp \to \bar{p}$	$q\bar{q}\to q\bar{q}$ $\bar{q}\to\bar{p}$	qM*→qM* M*→$\bar{p}$	$(1-x_T)^7$	$(1-x_T)^6$	$(1-x_T)^{5.4}$
	qq→qq q→$\bar{p}$	$q\bar{q}\to B^*\bar{B}^*$ $\bar{B}^*\to\bar{p}$	$(1-x_T)^7$	$p_T^{-4}(1-x_T)^2$	
pp→p	qp→qp	qB*→qB* B*→p	$p_T^{-4}(1-x_T)^{-4}$ (f)	$p_T^{-4}(1-x_T)^{-2}$	$p_T^{-3.2}$ $(1-x_T)^{-2}$
	qq→qq q→p		$(1-x_T)^3$		
	q(qq)→q(qq) (qq)→p (d)		$p_T^{-4}(1-x_T)^{-2}$ (f)		
$\pi^- p \to \pi^o$	qq→qq q→π^o	qM*→qM* M*→π^o	$(1-x_T)^{-3}$ (e)	$(1-x_T)^{-2}$	$(1-x_T)^{-1.6}$ (e)

Notes to Table 1

(a) x_T dependence of CIM calculated assuming M*, B* decay introduces no x_T factors. (See text.)

(b) CIM naturally predicts correct p_T and x_T dependence of $\pi^{o,+}$ production.

(c) Quark quark scattering must be adjusted to get p_T dependence; then x_T dependence is a correct prediction.

(d) Favored by a naive interpretation of associated multiplicity data - Section VI.

(e) See Fig. 5 to show that data agrees with quark quark scattering better than $(1 - x_T)$ power laws suggest.

(f) p_T, x_T dependence not clearly predicted.

(g) Data from Refs. 27, 28, and 29.

IV. Jet Cross-Sections

The Fermilab multiparticle spectrometer group has recently reported[30] very preliminary data which compares "jet" with single particle cross-sections. A "jet" is defined experimentally as a collection of particles in a restricted region of phase space the sum of whose transverse momenta is large. A calorimeter which is sensitive to both electromagnetic (π^0) and hadron ($\pi^{\pm}$..) showers was used in the trigger sketched below.

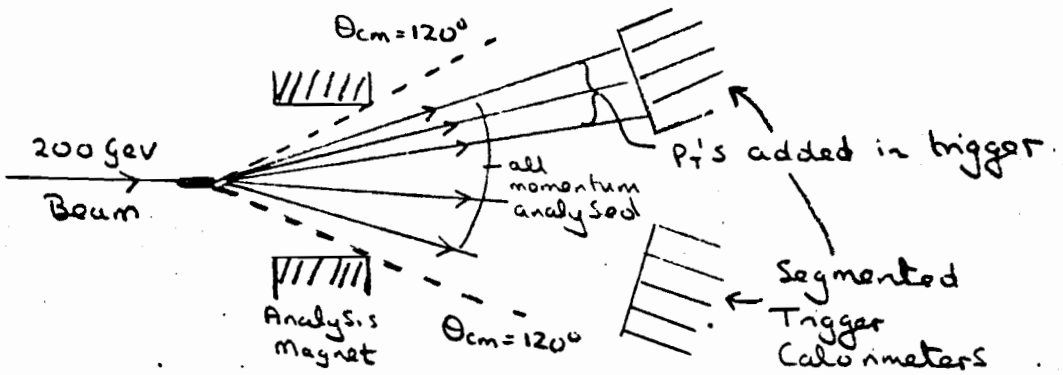

By using a single module of the four module segmented calorimeter one can simultaneously take data on jet and single particle triggers shown below

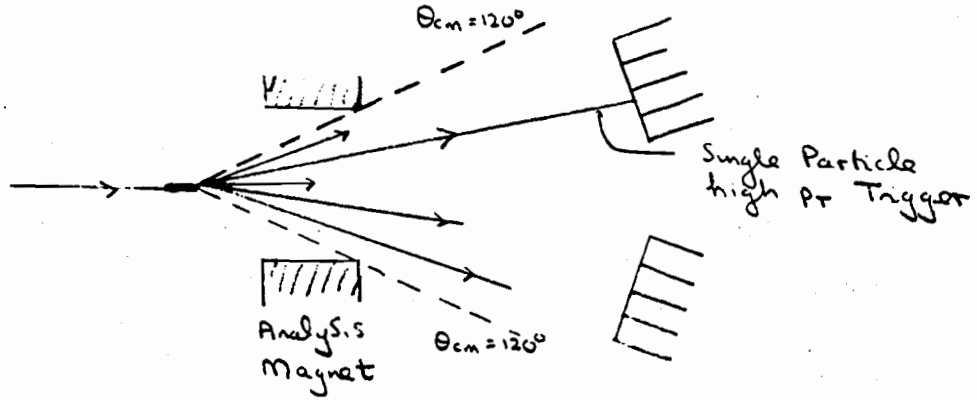

All charged particles with $\theta_{cm} \geq 90°$ are momentum analyzed while the acceptance drops to 50% at $\theta_{cm} \approx 110°$ and zero at $\theta_{cm} \approx 120°$. The general character of the data reported by this group are are summarized in Table 2. The exact definition of a jet is clearly subject to much debate but for a particular definition which is believed to underestimate number of jets (it only selects those jets whose charged particles have $p_T > .75$ GeV) they compare the away side distribution for single particle and jet triggers. Their results are shown in figure 7 and show a striking similarity between the two triggers. This data also allows one to measure the total jet cross-section: current results are consistent with the large value given by the quark model discussed in the next paragraph. However further analysis is needed before a firm number can be quoted.

Table 2: Fermilab MPS High-p_T Data (E260)

Reported analysis based on test run with Beryllium Target. Currently the group is working on further analysis of this and about factor of 10 more data with hydrogen target.
3160 single particle events with $p_T > 2$ GeV, $\langle p_T \rangle = 2.5$ GeV.
1068 jet events with $p_T > 2.75$ GeV, $\langle p_T^{jet} \rangle = 3.5$ GeV.
Mean rapidity (either trigger) = .25 .
Mean momentum analysed tracks per event = 9.5.

In the quark model Q, the single particle cross-section at a given p_T is some two orders of magnitude below the cross-section to produce a quark at the same p_T and this large factor can be easily understood as follows. A single particle always comes from a quark carrying more p_T (typically 20% more) than it. Further the probability of a quark to decay into a charged particle with $x_C \sim .8 \to .9$ is only a few percent. These two effects combine to give the result plotted in figure 8. Thus this model predicts the large jet cross-section suggested by the current E260 analysis. Further as illustrated in figure 1, both single particles and jets are accompanied by a quark fragmenting on the away side. In the "jet" case this quark has the same transverse momentum as the trigger jet p_T. So the x_e distribution (as defined in Fig. 2) should be essentially the same as observed in lepton processes (i.e. $p_{hadron/quark}(x_d)$) and shown in figure 3. For single particle case, the away side quark carries a fraction $1/x_C$ of single particle trigger p_T. Then we get $x_e = x_d/x_C$ and the estimate $\langle x_C \rangle = .85$ motivates the quantity plotted in figure 7. Including the internal transverse momentum (k_T) of the constituents reduces the theoretical estimate as described in II. The final predictions shown in figure 7 are in excellent agreement with experiment.

On the other hand it seems very hard to understand this data in a simple CIM model. First of all this model does not give a large jet cross-section: in fact it is naively equal to the single particle value summed over charges and particle types. Secondly, as illustrated in Fig. 1, a quark fragmentation should be observed on the away side for a single particle trigger; this is just like model Q. On the other hand, a jet trigger should be balanced on the away side by a single particle. This asymmetry, which seems basic to the model, is not observed in the data. Of course the general model C* which replaces the single particle by an arbitrary $q\bar{q}$ or qq system[35] has sufficient flexibility to fit the data.

Finally, we comment on mixed models like D of Section II, where single particle triggers come roughly equally from both CIM and quark-quark scattering terms. The jet trigger would only be sensitive to latter term and so this data is certainly consistent with such mixed models.

V. On the Same Side as the Trigger....

The fact that high p_T particles are not isolated but are just one member of an associated cluster of high p_T particles was evident before the jet trigger data of the previous section. Figure 9 shows the beautiful data[3,31,32] of the CCHK collaboration - this shows the rapidity spectrum of particles produced within a 25° azimuthal range of a high p_T trigger particle. A very striking peak is observed at the same rapidity as the trigger particle. Such behavior is certainly expected in the quark quark scattering model but in order to make quantitative predictions we must make the further assumption illustrated below:

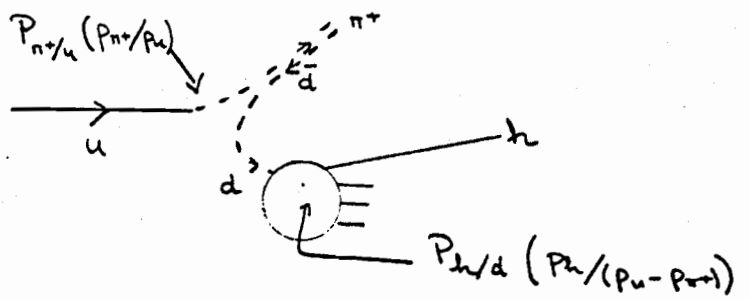

For example, when a π^+ is produced from a u quark we assume that the remaining hadrons in the jet can be calculated as the decay products of a d quark carrying the momentum of the original quark minus the trigger π^+. Essentially the same idea has been used many times before[7,8,33]. It would be very nice to check it using two particle correlation data in lepton processes e.g. e^+e^- → two hadrons plus anything. Experience[34] from similar ideas in

hadron hadron collisions would lead one to hope the assumption should be good to a factor of 2. Note that for a π^+ trigger, one looks at decay of d quark and so one will find more negative than positive hadrons in the associated particles. This is certainly not surprising or deep: however it is nice that our ansatz naturally has this feature. Figures 10 and 11 show a typical comparison of theory and experiment for the 45° negative trigger data. The agreement is better than one would have expected: the model gets the correct magnitude both as a function of p_T and the charge state i.e. the experimental ratio $h^+h^-/h^-h^- \sim 3$ is reproduced by the theory. The experimental 20° results are also well reproduced: the lower associated multiplicity at 20° shown in figure 9 is cleanly predicted as the mean value of x_c automatically increases to reflect the more rapid fall off with p_T of the invariant cross-section. The lower correlation makes the background subtraction harder: further at 20° in the low $p_T(\lesssim .5$ GeV/c) region, the theory is very sensitive to the frame used. So far we have assumed that all x's are defined in the original hadron c.m.s.: this is not obviously correct. We will return in a later paper[17] both to the frame ambiguity and also to change in background expected when high momentum quark is removed as is the case with small angle triggers.

The quark quark scattering model Q is also successful in predicting the energy dependence of the towards correlation data shown in figure 12. This comes from the CCRS collaboration[29] and is a measurement of the charged particles produced in association with a single particle π^o trigger at 90°. The energy dependence comes in the model from the decreasing mean x_c with increasing energy which reflects the gradual flattening of the single particle p_T distribution with increasing energy.

We now turn to other models. This type of data cannot be understood in the basic CIM model C. In the generalized model C*, the associated particles are just the remaining decay products of the (resonant) M* or $q\bar{q}$, qq system[35] produced in the hard scattering $qM^* \to qM^*$. One can say little in the absence of a quantitative formulation but the success of the quark model Q indicates that it may not be easy to find an attractive CIM model. Thus one might guess that agreement with the data (especially the like charge correlation) will require an $M^* \to h$ decay function (P_{h/M^*}: h is trigger hadron) similar to the quark decay $P_{h/q}$ of model Q. As discussed in Section III, this might spoil the successful single particle cross-section predictions. (It changes power of $(1 - x_T)$). Further a naive analogy between P_{h/M^*} and inclusive $\pi^- p \to \pi$ hadronic reactions would not lead one to expect that P_{h/M^*} had the same small probability of producing high $x \gtrsim .8$ hadrons as shown by quarks.

VI. Associated Multiplicity Distributions

Many groups have reported data on the associated multiplicity of charged particles produced in conjunction with a high p_T trigger. I will use the new data[36] of the DILR collaboration which has separate distributions for each species of trigger particle. This is important because in all the models the different mechanisms (i.e. basic 2 → 2 hard scattering amplitudes), typified in Table 2, should lead to rather different correlation phenomena for each trigger species. Even when the 2 → 2 amplitude is the same (e.g. qq → qq in model Q) the different x dependence of $P_{\pi/q}$ and $P_{p/q}$, for instance, leads to easily observable differences between the associated multiplicity with pi and proton triggers. Associated multiplicity is by no means the only correlation measurement sensitive to trigger species: it just happens to be the only data available to me at present.

The DILR group fit their multiplicity data to the empirical form

$$M_h(\phi, p_T, \sqrt{s}) = A_h(\phi) + B_h(\phi)p_T + C_h(\phi)\ln(s/s_o) \quad , \qquad (4)$$

$$\sqrt{s_o} = 44.7 \text{ GeV} \quad ,$$

where h denotes trigger species and ϕ is the normal azimuthal angle defined in Fig. 2. The easiest (and largest) term in (4) to understand is B_h: the coefficient of p_T. This directly reflects the contribution of the constituent fragmentation.

For ϕ ~ 180° we see the away side d, and for ϕ ~ 0 the towards side. The latter is of course much smaller as the trigger particle has taken most of the constituent momentum; crudely speaking (ignoring longitudinal components) ϕ ~ 180° is sensitive to decay with momentum $p_T^{constituent} \sim p_T^{trig}/\langle x_C \rangle$ and ϕ ~ 0° to $(1 - \langle x_C \rangle)\ p_T^{trig}/\langle x_C \rangle$. In figure 14 we compare model Q for a π trigger with the experimental B_π for three ϕ ranges (~0, ~90 and ~180°). There is a slight problem as the theory does not predict the linear p_T dependence given in (4) but rather the standard $\ell n\ (p_T)$ behavior. This is not a contradiction as it is well known in hadron hadron collisions that logarithmic dependence for multiplicity does not set in until high incident energy. However it does make comparison of theory and experiment harder: in Fig. 14 we simply calculated the theory at three p_T values (2,3 and 5 GeV) and drew a line of slope equal to experimental B_π through the p_T = 2 theoretical point. Theory and experiment agree quite satisfactorily for ϕ ~ 0 and 180°. This confirms two main points: first, on the away side, that the fragmentation of d does have, as predicted, a multiplicity similar to that seen in e^+e^- annihilation and other lepton processes. Secondly, on the towards side, that the mean $\langle x_C \rangle$ of model Q is about right: we drew the same conclusion from the CCHK data in the last section. Turning to the CIM model, it appears likely that any generalization consistent with the jet and towards correlation data discussed already, will also be able to give fits to the DILR data comparable to those in Fig. 14 for model Q.

Now we turn to fine details of the DILR data. At present I do not understand fully the non zero value of $B_\pi(\phi \sim 90°)$: thus in Fig. 14, theory does not predict the increase with p_T of 90° multiplicity seen in the data. The p_T independence of the theory corresponds to a p_T independent dx/x distribution for quark decay. Now the analogous assumption for hadron-hadron collisions, i.e. energy independent height of rapidity plateau, is certainly not true - a marked rise with energy being observed which persists even at ISR energies[37]. If quark decay

had a similar non scaling behavior, B_h (90°) will also increase by an amount I estimate is within a factor of 2 of the experimental observtion. The s dependence observed by DILR (i.e. the coefficient C_h in (4)) is in a comparable state: a more detailed investigation is needed to decide if it is anything more than non scaling of constituent decay functions.

The particle species dependence of the DILR data is more directly interpretable: for instance the larger B for antiprotons triggers would follow if $\langle x_C \rangle$ is smaller than for π's. This is true, in model Q, if $\bar{p}$'s come from quarks or antiquarks. In model C*, $qM^* \to qM^*$ ($M^* \to \bar{p}$) would certainly give lower $\langle x_{\bar{p}} \rangle$ than $\langle x_\pi \rangle$: on the other hand $q\bar{q} \to B^*\bar{B}^*$ would not. As Table 1 shows, the single particle data also supports the $qM^* \to qM^*$ mechanism favored by the multiplicity data. Apart from antiprotons, the other trigger species have roughly the same $B(\phi)$ and hence the same $\langle x_C \rangle$ in constituent models. Perusal of Table 1, suggests this would be predicted by the CIM model but that proton production is a problem for model Q. The generalized mechanism $q(qq) \to q(qq)$, with diquark $(qq) \to$ proton would very naturally give $\langle x_p \rangle \simeq \langle x_\pi \rangle$ and agreement with data. On the other hand, one would rather maintain the simplicity of the model and only use

$$qq \to qq \ , \ q \to p \qquad (5a)$$

$$qp \to qp \ , \ \text{leading particle term} \qquad (5b)$$

A simple $(1 - x)^3$ for $q \to p$ gives $\langle x_p \rangle$ ~ .67 as opposed to $\langle x_\pi \rangle$ ~ .82 at p_T = 3 GeV. This leads to an increased multiplicity associated with proton triggers as is summarized in Table 3 which also gives the term (5b) with its simple $\langle x_p \rangle$ = 1.

Table 3: Associated Multiplicities at $p_T^{trigger}$ = 3 GeV, $\sqrt{s}$ = 44.7 GeV

Term	ϕ Range	Proton Minus π trigger Multiplicities in ϕ cut.
(5a)	$\lvert 180 - \phi \rvert \leq 36°$	.31
(5b)	"away"	-.4
Expt		.25
(5a)	$\lvert \phi \rvert \leq 36°$	.49
(5b)	"towards"	-.55
Expt		.25

It is possible that a combination of (5a) and (5b) will fit the data: we must await the future. In any case it is clear that the trigger species dependence (especially p v. $\bar{p}$ v. meson) of correlation data will be a valuable constraint on model building.

VII. On the Other Side: Shape of the Rapidity Distribution

Our discussion of the away side divides naturally into the angular dependence, discussed here, and the magnitude of the momenta discussed in the the following section. We will again use the new CCHK experiment[31] and this time the data is shown in Fig. 15. In figures 16 and 17 we show typical predictions for model Q at 20° and 45°. The agreement is not spectacular: the theory is both larger and narrower than the data. However theory and experiment both exhibit the same striking independence of the away side distribution with trigger rapidity: again even for the 20° trigger (rapidity 1.9) the away side distribution is still (roughly) centered at rapidity zero. The latter feature is an important success of the model as is shown by Fig. 18

which compares the away side rapidity shapes for the same quark probabilities $P_{q/h,h/q}(x)$ but the different scattering amplitudes:

vector gluon exchange: $d\sigma/d\hat{t} = (\hat{s}^2 + \hat{u}^2)/(\hat{s}^2\hat{t}^4)$. (5a)

Field-Feynman: $d\sigma/d\hat{t} = 1/(-\hat{s}\hat{t}^3)$ (5b)

$d\sigma/d\hat{t} = 1/\hat{s}^4$ (5c)

For (5a), configurations with small $\hat{t}$ are emphasized and one obtains the back to back situation of Fig. 18 with an away peak at negative rapidities for a trigger at positive rapidity. For (5c), small $\hat{s}$ is achieved by the "back anti-back" phenomena with an away peak at positive rapidity for positive rapidity trigger. The intermediate Field/Feynman amplitude (5b) is roughly symmetric about y = 0 in agreement with experiment. It is interesting that the empirical form (5b) was in fact chosen to agree with the observed angular distribution on the trigger side: this same choice then gives the correct angular distribution on the away side.

We now turn to the width of the rapidity distribution. The theory so far has been calculated using x variables defined in pp center of mass. As an extreme illustration of the sensitivity of our results to this assumption, we calculated the prediction using the x for quark d decay defined in quark-proton c.m.s. (taking "nearest" proton to quark).

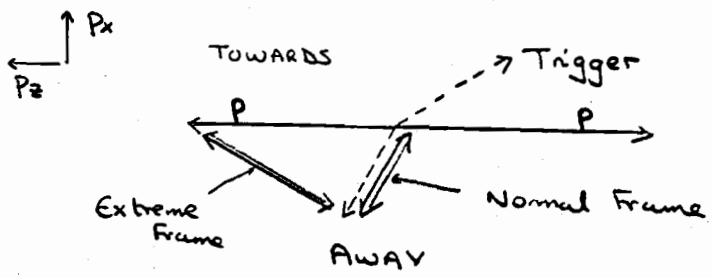

Figure 19 shows that even for $p_T > 1$ GeV on the away side this extreme frame produces a large change. The effects at lower p_T or for 20° trigger are even larger. Use of more reasonable frames, e.g. quark c - quark d or quark-"hole" c.m.s.[38] produces much smaller changes. One might imagine that the distributions seen in the data of Fig. 15 to be broader for positive than negative particles could be connected with finding the right frame theoretically.

We now turn to the magnitude of the distributions. As is clear in Figs. 16 and 17, the theory is typically larger than the data. We can try to summarize the comparison by integrating over the away side rapidity. The results are presented in Table 4 below.

Table 4: Normalization of Away Side Rapidity Distributions for Quark Quark Scattering

Condition	Theory/(Experiment-Background)
Total	1.3
all 45°	1.35
all 20°	1.2
all $.3 < p_T^{away} < .5$ GeV	1.35
$.5 < p_T^{away} < 1$ GeV	1.1
$p_T^{away} > 1$ GeV	1.4
all + trigger charge	
+ negative secondary	1.2
charge (+ + -)	
- + -	1.45
- + +	1.1
+ + +	Rapidity range of expt not complete

Rather than give all 24 ratios implied by the angle/trigger charge/secondary charge/p_T range combinations of Fig. 15, I have given in the table above just some of the significant subtotals: for instance, line 1 in the table above means that averaged over all combinations the theory is 30% higher than the experiment. The latter has the minimum bias background, given in Fig. 15 as a solid line, subtracted from the data points. From the p_T dependence of the normalization we see that the theory is even somewhat better at low $p_T < 1$ GeV (where it is least reliable) than it is at high p_T. This disagreement at high p_T will be studied more quantitatively in next section where we note that the theory will go down in size if you increase mean $\langle k_T \rangle$ of quarks in hadrons but will go up if you use one of the other frames (e.g. quark-"hole") discussed above. An interesting consequence of the agreement of the theory for low p_T associated particles both here and in the towards correlations of the last section is that it justifies the simple idea of adding the high p_T and normal secondaries. This leads to a rapidity plateau sketched below[38] that is double the size in high p_T as in normal reactions.

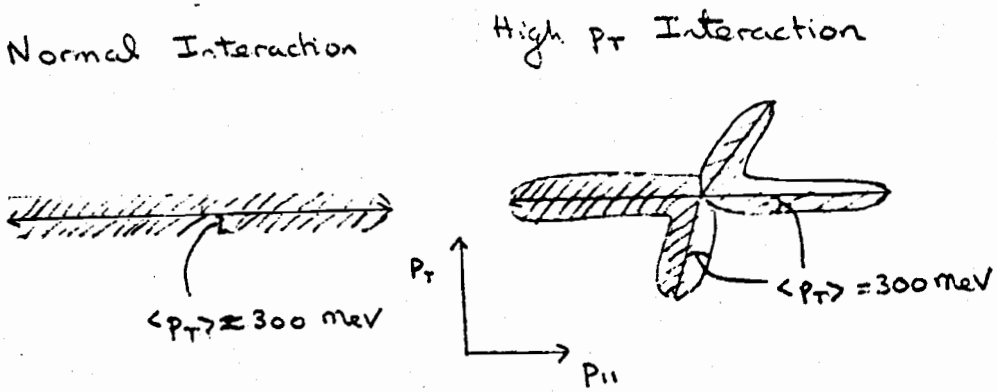

This picture has been partially tested by the Pisa Stonybrook collaboration[39].

Returning to Table 4, we note that the data show more positive than negative charged hadrons on the away side whether the trigger has + or - charge. Model Q agrees qualitatively with this observation although there is a slight quantitative mystery. Thus experimentally the ratio of $(+ \to +)/(+ \to -)$ is smaller than $(- \to +)/(- \to -)$ whereas theory gets similar values for both ratios. It appears that the $(- \to -)$ configuration at 20° is suppressed experimentally: it will be interesting if this effect is confirmed.

Turning to the CIM model, we remember from Fig. 2 that it, just like model Q, has a quark fragmenting on the away side. So we will not find the dramatic differences between the two models on the away side that we found with the towards correlations. Table 5 summarizes the situation: the first point concerns the normalization of the away side. Given the virtual necessity of the generalized model C* which will presumably have a similar $\langle x_C \rangle$ to model Q, it appears reasonable to say that both models (CIM and quark quark scattering) give the same prediction for normalization on the away side.

Table 5: Differences Between CIM Model and Quark-Quark Scattering on the Away Side

Theoretical Feature	Experimental Consequence
(a) x_C naive CIM = 1, $\langle x_C \rangle$ ~ 0.8 in model Q	Normalization of away side lower in CIM model. However, generalized model C* probably similar to model Q.
(b) $\hat{s},\hat{t}$ dependence of force	Shape of old CIM (model C) away side is "back anti back." New version of CIM gives same force as model Q and agrees with experiment. Model C* gives ?
(c) Type of towards and away side quark uncorrelated in model Q. Specific diagrams lead to correlations in model C.	Model Q, +/- charges on away side always > 1 as more u's than d in proton. In CIM +/- depends on trigger configuration.

The next two points ((b) and (c)) in Table 5 concern the details of the CIM hard scattering amplitude: let us first use the normally quoted form[6,21] for this amplitude. Namely for high p_T π production we have typically

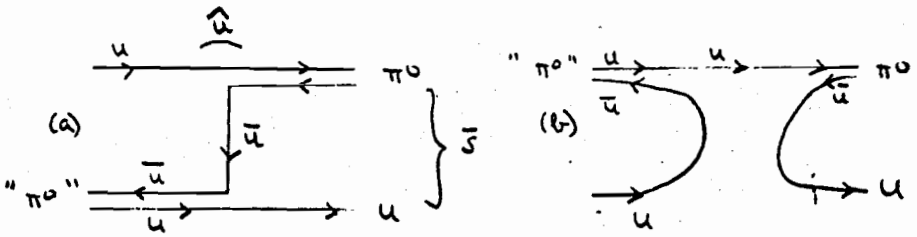

(a) $\hat{t}$ channel exchange: $\frac{d\sigma}{d\hat{t}} = \frac{1}{\hat{s}^2\hat{u}^2}$ (6a)

(b) $\hat{s}$ channel pole: $\frac{d\sigma}{d\hat{t}} = \frac{1}{\hat{s}^4}$ (6b)

(c) coherent sum: $\frac{d\sigma}{d\hat{t}} = \frac{1}{\hat{s}^2}\left(\frac{1}{\hat{s}} \pm \frac{1}{\hat{u}}\right)^2$ (6c)

where the different quark, π type/charge choices lead to (6a,b,c). An explicit calculation, summing over all possibilities, gives the away side rapidity shape shown in Fig. 18: the "back anti-back" prediction of this version of CIM model clearly disagrees with experiment. It has recently been pointed out[40] that (6a,b) are appropriate to spin 0 quarks and it is more reasonable to replace them with $1/(-\hat{s}\hat{u}^3)$ and $(-\hat{u})/\hat{s}^5$ respectively which correspond to spin 1/2 quarks. Such a $d\sigma/d\hat{t}$ will agree with the rapidity shape of the current data. In fact the prediction of the correct angular dependence of $d\sigma/d\hat{t}$ is an important success of the spin 1/2 CIM model.

The prediction of CIM model for charge ratios on the away side is much more subtle than in model Q: the latter has essentially no correlation between away and same side. On the other hand, CIM quark exchange carries non trivial quantum number correlations between the away and towards sides. A detailed discussion has not been given and a proper experimental test demands determination of particle species on both sides. However let us take a brief look starting with 90° π^o triggers. In this case the π^o target diagrams on the previous page are suppressed because of destructive interference in the coherent sum (6c). Dominant are

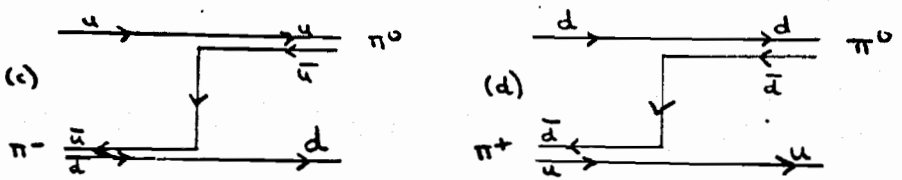

Summing these leads to more negative than positive away side particles as diagram (c) is enhanced by the larger u than d structure function in the proton. Explicitly for a 2.5 GeV/c π^o trigger, CERN R412 finds[22] + charge/ - on the other side = 1.3. This agrees with model Q but the above CIM calculation gives a ratio of .92. Again consider the charged triggers of the CCHK collaboration[31] and ignore all species except pions. For π^- trigger, we get two important diagrams

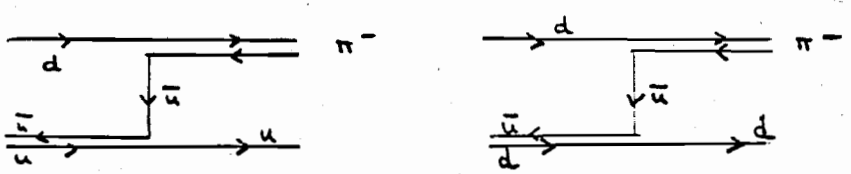

For equal $\bar{u}u$, $\bar{u}d$ components in proton, one finds +/- charges = 1 on other side in disagreement with experiment. One can try to repair model by making very reasonable assumption that

$$(\bar{d}u) > (\bar{d}d),\ (\bar{u}u) > (\bar{u}d) \quad \text{in proton} \tag{7}$$

Unfortunately putting all $\bar{q}q$ components equal gets about the right ratio for π^+/π^- single particle cross-sections (the correct value coming from different u/d structure functions). Imposing (7) would increase the π^+/π^- single particle production ratio above the experimental value.

I might also remark here that the quark fusion model[9,15,24], i.e. dominant hard scattering is $\bar{q}q \to M^*M^*$ (M^* decays into hadrons as in model C*), seems to have difficulty understanding the away side charge ratios in CCHK experiment[31]. Surely this model would predict +/- on the away side is smaller for a positive than a negative charge trigger? The data do not seem to show this. Combridge has also shown that the same model gets too large a value for π^o production from a π^- beam[41].

Enough of these detailed arguments: it is important to search experimentally and theoretically for reliable quantum number correlations in the CIM model. Observation of them would be very important evidence for the basic soundness of the model in spite of the unfortunate complication shown by the necessary generalization C*.

VIII. On the Other Side: $d\sigma/dx_e$ Distribution (See Fig. 2 for definition of x_e)

We have already discussed distributions in x_e in Section IV where we compared jet and single particle triggers. The first data of this sort came from the CERN R412 experiment[22] which used a π^o trigger with a mean p_T of 2.5 GeV. Their results are compared with model Q in Fig. 20: the theory has a reasonable shape but is a bit high. Using a mean internal transverse momentum of 500 MeV

as opposed to the conventional 330 MeV gives much better agreement as shown by the dotted line in Fig. 20. The data of Fig. 5 indicates it would have been more precise to use 330 MeV for $P_{h/q}$ and the larger value for $P_{q/h}$. This also agrees with experiment. Note that the high $\langle k_T \rangle$ calculation is very sensitive to the extrapolation of hard scattering amplitude to low values of the invariants $\hat{s}$, $\hat{t}$, $\hat{u}$. The current calculations have an artificial cut off to cope with this problem: removing this would significantly (~25%) decrease away side curve in Fig. 20 for $\langle k_T \rangle \simeq 500$ MeV. On the other hand increase of a comparable amount is found using the different frames discussed in previous section. Within the above uncertainties, we conclude that model Q is in agreement with the CERN R412 x_e measurements.

Figure 21 compares the distribution in p_{out} (cf. Fig. 2 for definition) for theory and experiment. The larger $\langle k_T \rangle$ is clearly preferred although it must be emphasized that no background has been subtracted from the data: any subtraction must sharpen experimental curve. Note that the x_e independent mean p_{out} quoted in the experiment is not expected theoretically. Thus when the quark d decays, all the internal transverse momentum smearing is scaled by $x_d = x_e$ except that due to the final decay of d. This leads to (approximate) expectation

$$\langle p_{out} \rangle = \sqrt{\sigma_1^2 x_e^2 + \sigma_2^2 (1 + x_e^2)/2} \qquad (8)$$

where σ_1 is mean internal transverse momentum of quarks in hadrons and σ_2 for hadrons from quarks. The properly calculated theory is compared with experiment in Fig. 22 for $\sigma_1 = \sigma_2 = 330$ MeV. Increasing σ_1 will only increase x_e dependence although (as illustrated) it does improve agreement. It is not clear if x_e independent p_{out} seen experimentally is a real effect or just a consequence of limited eptance and/or lack of background subtraction.

In Fig. 23 we show again that model Q gets the correct shape but

too large a magnitude - this time comparing it with the CCRS data[29]. This prediction is particularly sensitive to $\langle k_T \rangle$ as the acceptance of charged particle spectrometer was rather small. A larger $\langle k_T \rangle$ will again bring agreement between theory and experiment. Figure 23 also shows the minimum away side prediction - namely that for a delta function trigger $x_C = 1$. It agrees nicely with experiment for $\sigma_1 = \sigma_2 = 330$ MeV. This is of course the naive CIM model C prediction but the generalized model C* demanded by other correlation data, probably looks very similar to model Q. The better agreement of the away side magnitude using a delta function decay led Ellis et al.[8] to propose a substantial contribution from such a term to the single particle trigger. The situation is not yet clear but it is my feeling that the agreement of model Q with the towards correlation weakens the case for the delta function term: the size of the away side cross-section can be more plausibly lowered by an increase of $\langle k_T \rangle$ for quarks in hadrons. One might hope to test delta function model by looking at the towards correlation for events which show large x_e. As pointed out by Jacob and Landshoff[33] this will enhance the non delta function term and lead to an increased towards correlation. Unfortunately Fig. 24 shows that the bare model Q has the same effect: the towards correlation quadruples as you go from all events with one particle with $x_e > .15$ to those with $x_e > .75$.

We would like to finish with a particularly devastating piece of data. The CCHK collaboration shows[4] that the $d\sigma/dx_e$ distribution is not independent of the trigger p_T : in fact they find a factor of three drop in the away side cross-section as they change trigger p_T from $2 < p_T < 2.3$ to $p_T > 3$ GeV. This data shown in Fig. 25 is compared both with the normal model Q and the delta function decay discussed above: in each case the theory has essentially no dependence on trigger p_T. Again all versions of the CIM model (C or C*) will have the same qualitative disagreement with the data as seen for quark quark scattering. Increasing the internal transverse momentum $\langle k_T \rangle$ decreases $d\sigma/dx_e$

but in a trigger p_T independent way. If this data is confirmed, (all) theories will have to be substantially changed. As for fixed parameters, $d\sigma/dx_e$ is independent of p_T we must arrange for some parameters in the theory to change with increasing p_T. One possibility, is $\langle k_T \rangle$: another is offered by the possibility, anticipated at the end of Section II, of constituents in the proton which have a smaller probability to give high $x \geq .5$ hadrons than normal quarks. We will call these constituents gluons, although charmed or other exotic quarks would lead to similar effects. Gluons would not effect the towards side as this is only sensitive to $x_C \geq .6$ and by assumption gluons do not give hadrons in this high x_C region. However, on the other side, you see the gluon decay without suppression. Now we arrange our parameters so that quark-quark scattering dominates $p_T \sim 2.5$ GeV triggers while quark-gluon scattering takes over at higher p_T. Agreement with experiment ensues. A similar ruse is no doubt possible in the CIM framework. All this is rather far fetched at present and we must await further experimental work.

IX. Conclusions

The evidence for constituent models of high p_T scattering is now very striking. Essentially all features of the single particle and correlation data are understood semi-quantitatively. Theoretically the situation is challenging for fundamental field theory has yet to justify this approach with its close quantitative relation between lepton and hadron processes. There are many new experiments being analysed now which will allow more precise tests of the theory. In a year or so the situation will become much clearer.

The models we have now are clearly oversimplified and unlikely to be right in any absolute sense. However it seems very valuable to explore the predictions of simple well defined models: hopefully this will lead to precise statements of simple phenomena which are to be explained by fundamental theory. We considered two main models: the quark quark scattering model and the generalized constituent interchange model C* give comparable fits to current data. The quark model gives

a simple and good fit to the towards correlation data: CIM models fit the same data only by letting resonances decay into single particles in a similar manner to quarks. On the other hand the CIM model explains more naturally the proton inclusive cross-section and associated multiplicity. Both models give similar fits to the "away" side distributions: internal transverse momentum smearing is important in understanding this data. However there is as yet no clean way of understanding the CCHK data showing non scaling of the x_e distribution.

In Table 6, we summarize the basic models with possible extensions, and list some of their critical phenomenological features. Further experimental investigation of this is obviously critical. Phenomenologically it would be nice to quantify the CIM model and to extend it and/or the quark model to a complete picture of the interaction - both high p_T particles and "background."

Acknowledgements

I would like to thank R. D. Field and R. P. Feynman with whom much of the work described here was done. Discussions with S. Ellis, G. Farrar and M. Gell-Mann have been very enlightening. Finally I am grateful to the members of the Fermilab MPS collaboration, especially Jerry Pine, for welcoming an ugly duckling into their midst.

Table 6: Summary of Constituent Models

Model	Reference	Typical Hard Scattering Reaction	Points to Watch
Q	Ref. 16	$qq \to qq$	p_T and angular dependence of amplitude taken from experiment. Proton production not predicted yet. Large jet cross-section. Towards side correlations good. CCHK $d\sigma/dx_e$ non scaling mysterious.
C(CIM)	Ref. 10	$q\pi \to q\pi$	p_T and angular dependence of amplitude (correctly) predicted. All single particle cross-sections predicted reasonably. Small jet cross-sections. Towards side correlations bad. CCHK $d\sigma/dx_e$ non scaling mysterious.
Q*	Section II, here	Q plus $q(glue) \to q(glue)$	Maybe helps away side fits of model Q including $d\sigma/dx_e$ non scaling but not obviously needed.
Q*	Section II, here	Q plus $q(qq) \to q(qq)$	Maybe explains proton production but not obviously needed.
C*	Section II, here & Ref. 35	$qM^* \to qM^*$ or	Maybe cures towards and jet problems in C.
		$q(qq) \to q(qq)$	Away side as model Q.
		$q(q\bar{q}) \to q(q\bar{q})$	Not clear if retains single particle predictions of model C.
D	Ref. 8	$qq \to qq$ and $q\pi \to q\pi$	Same comments as Q.
Quark Fusion	Ref. 9	$q\bar{q} \to M^*\bar{M}^*$	Problems with π/proton beam ratio. Away/towards charge correlation prediction poor.

References

1. H. Frisch, proceedings of this conference.
2. L. Di Lella, Review talk at 1975 International Symposium on Lepton and Photon Interactions at High Energies, Stanford,
3. M. Della Negra, Large Transverse Momentum Phenomena, Tutzing Conference, (1976).
4. R. Sosnowski, Correlations in Collisions with a High $p_\perp$ Particle Produced, CERN/EP/PHYS 76-56, Tbilisi talk (1976).
5. P. Darriulat, Large Transverse Momentum Hadronic Processes, Tbilisi talk (1976).
6. D. Sivers, S. Brodsky and R. Blankenbecler, Phys. Reports, 23C, 1 (1976).
7. J. D. Bjorken, Lectures delivered at the SLAC Summer Institute on Particle Physics, July 1975.
8. S. D. Ellis, M. Jacob and P. V. Landshoff, Nucl. Phys. B108, 93 (1976).
9. P. V. Landshoff, Large Transverse Momentum Jets: A Theoretical Review, Tutzing Conference (1976).
10. S. J. Brodsky and J. F. Gunion, Recent Developments in the Theory of Large Transverse Momentum Processes, SLAC-PUB-1806 (1976).
11. S. M. Berman, J. D. Bjorken and J. B. Kogut, Phys. Rev. D4, 3388 (1971).
12. J. D. Bjorken, Phys. Rev. D8, 3098 (1973).
13. S. D. Ellis and M. B. Kislinger, Phys. Rev. D9, 2027 (1974).
14. R. Blankenbecler and S. J. Brodsky, Phys. Rev. D10, 2973 (1974). See Ref. 6 for further CIM references.
15. P. V. Landshoff and J. C. Polkinghorne, Phys. Rev. D10, 891 (1974).
16. R. D. Field and R. P. Feynman, Quark Elastic Scattering as a Source of High Transverse Momentum Mesons, CALT-68-565 (1976).

17. R. P. Feynman, R. D. Field and G. C. Fox, preprint in preparation.

18. R. Hwa, A. J. Speissbach and M. Teper, Phys. Rev. Letters 36, 1418 (1976). This paper tries to motivate a modified quark quark model from scale breaking effects: their angular distribution differs from (2) and will not agree with experiment.

19. A. P. Contogouris and R. Gaskell, Large p_T Correlations in a Scale-Breaking Constituent Model, preprint (1976).

20. R. Baier et al., Hadronic Correlations at Large Transverse Momenta in the Parton Model, Bielefeld preprint BI-TP 76/25 (1976).

21. R. O. Raitio and G. A. Ringland, A Phenomenological Analysis of High p_T Spectra and Angular Multiplicity Correlations in pp Collisions, SLAC-PUB-1620 (1976). R. Raitio, Large p_T Hadron Physics: Gluon or Quark Exchange, preprint (1976).

22. P. Darriulat et al., (CERN R412 Experiment) Nucl. Phys. B107, 429 (1976).

23. S. Brodsky and G. Farrar, Phys. Rev. D11, 1309 (1975).

24. B. L. Combridge, Phys. Rev. D12, 2893 (1975).

25. L. Lederman, proceedings of this conference.

26. M. G. Albrow et al., (CHLM collaboration) Nucl. Phys. B108, 1 (1976).

27. G. Donaldson et al., Phys. Rev. Letters 36, 1110 (1976).

28. M. Schochet et al., Tbilisi conference report and H. Frisch in these proceedings (Ref. 1).

29. F. W. Busser et al., (CCRS collaboration) Nucl. Phys. B106, 1 (1976).

30. Fermilab Multiparticle Spectrometer Group, Comparison of Single Particle and Jet Production at High Transverse Momentum, preprint in preparation.

31. M. Della Negra et al., (CCHK collaboration), General Characteristics of Events with a Particle of Large Transverse Momentum in pp Collisions at $\sqrt{s}$ = 52.5 GeV, CERN/EP/PHYS 76-43, Tbilisi preprint (1976).

32. I apologize to the many other authors of correlation data that I have ignored in this review. I have just selected data that tests theory most precisely.

33. M. Jacob and P. V. Landshoff, Trigger Bias in Large p_T Reactions, CERN-TH-2182 (1976).

34. E. L. Berger and G. C. Fox, Phys. Letters 47B, 162 (1973).

35. J. C. Polkinghorne, Phys. Letters 60B, 281 (1976). This proposes a generalization of CIM where meson is replaced by $\bar{q}q$ or qq systems. This is essentially what I call model C*.

36. B. Alper et al. (DILR collaboration), multiplicities associated with the production of pions, kaons or protons of high transverse momentum at the ISR, preprint RL-76-031 (1976).

37. B. Alper et al. (British Scandinavian collaboration), Nucl. Phys. B100, 237 (1975).

38. R. Savit, Phys. Rev. D8, 274 (1973).

39. R. Kephart et al., (Pisa-Stonybrook collaboration) Charged Particle Multiplicities Associated with Large Transverse Momentum Photons, preprint (1976).

40. W. Furmanski and J. Wosiek, Single-Particle Inclusive Distribution at Large p_T in Parton Models, TPJU-8/76 Cracow preprint (1976).

41. B. L. Combridge, Phys. Letters 62B, 222 (1976).

42. G. Hanson, talk delivered at the SLAC Summer Institute, 1975.

43. K. J. Anderson et al., Production of Continuum Muon Pairs at 225 GeV by Pions and Protons, preprint (1976).

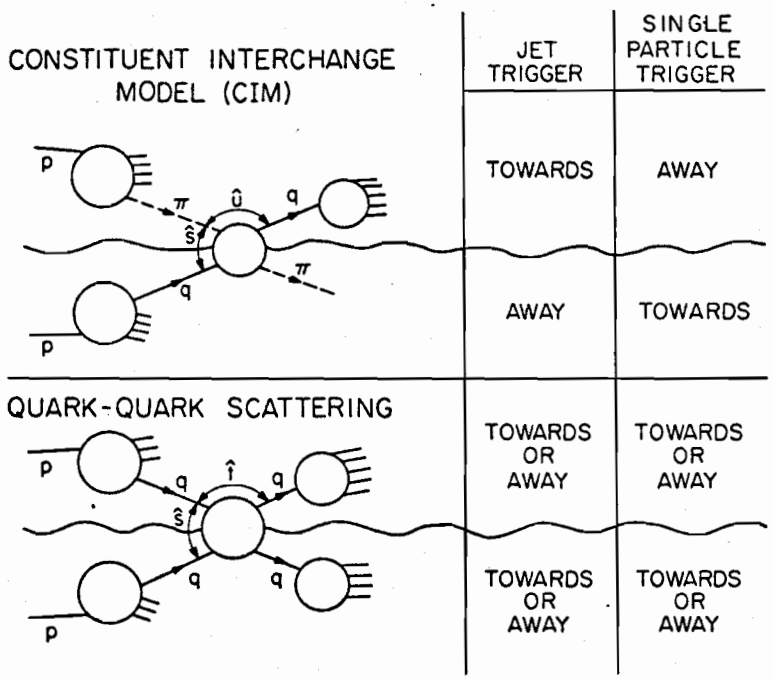

Fig. 1: The CIM (model C) and quark quark (model Q) scattering theories and their structure for jet and single particle triggers.

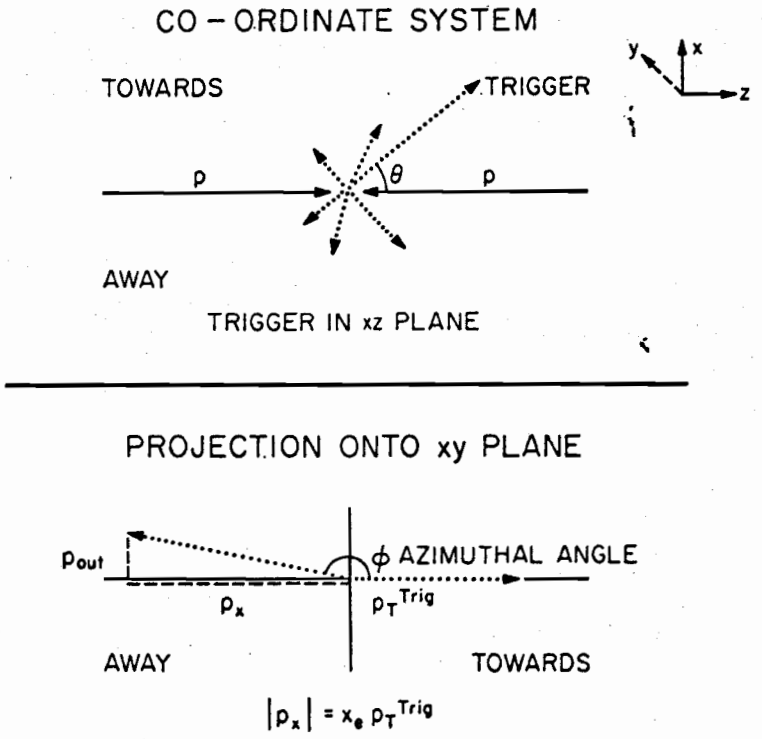

Fig. 2: The co-ordinate system used to describe high p_T production in pp collisions.

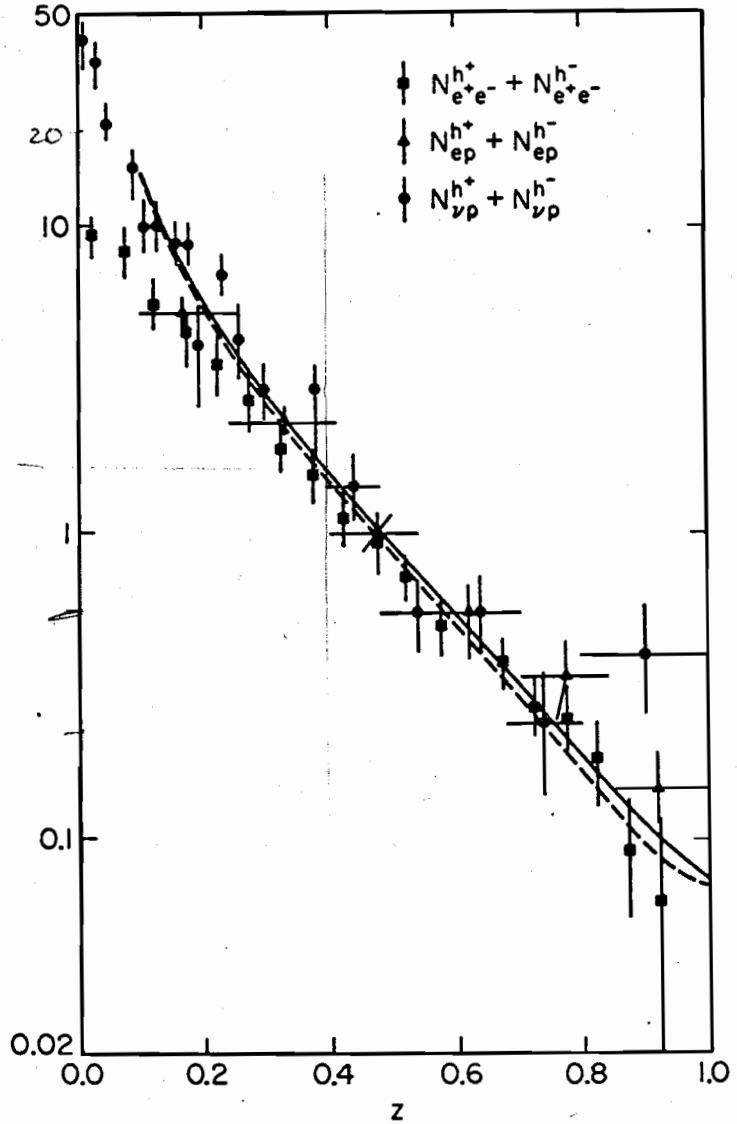

Fig. 3: Comparison[16] of three separate experimental methods of finding $P_{h/q}(z)$. The three different lepton processes differ slightly because they weight quark types differently. The solid line is the Field Feynman parameterization for neutrino case and dashed is e^+e^-: electroproduction lies between these two.

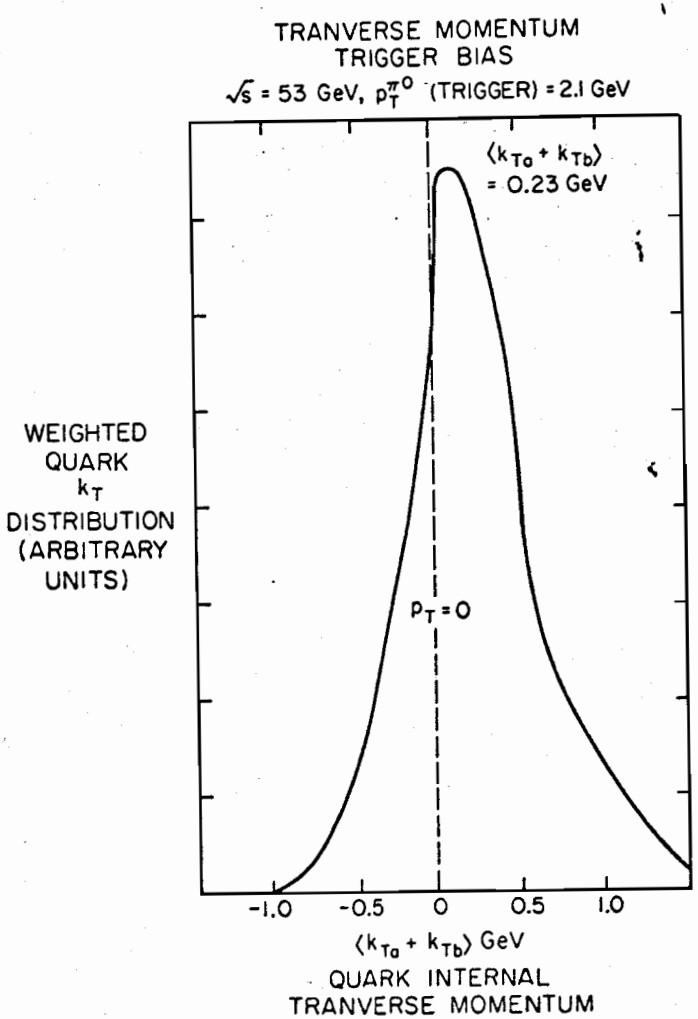

Fig. 4: Shows bias discussed in section II. Quark transverse momenta are pulled towards trigger particle. Input was an $\exp(-6k_T)$ distribution for each quark.

INTERNAL TRANSVERSE MOMENTA

HADRONS IN QUARKS

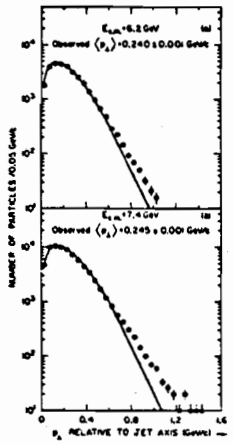

Fit
corresponds
to
$\langle k_T(h/q)\rangle = 315$ MeV/c

QUARKS IN HADRONS

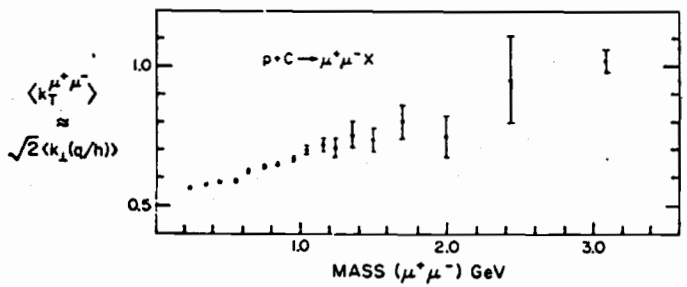

Fig. 5: Shows experimental evidence for internal transverse momenta of hadrons in quarks[42] (top) and quarks in hadrons[43] (bottom).

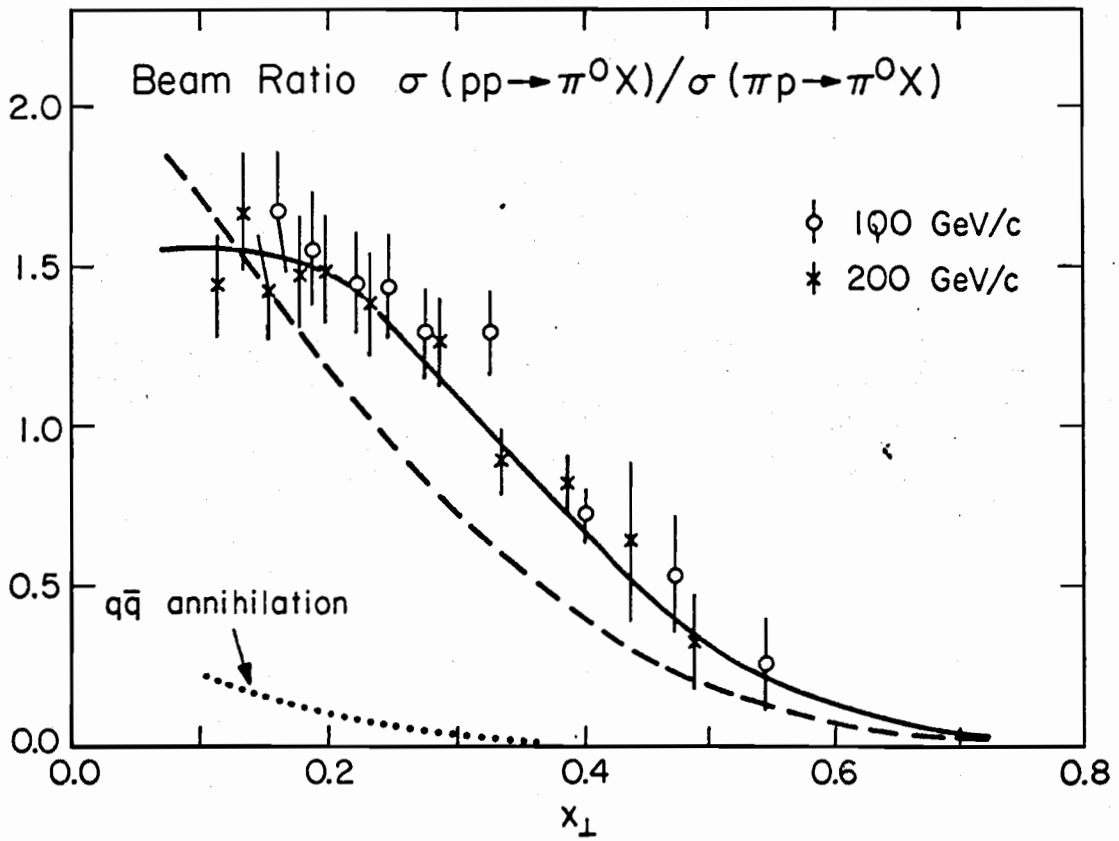

Fig. 6: Comparison of Field Feynman model (solid curve) with experimental data[27] on ratio of π^0 production at 90° with proton and pi beams. The dashed and dotted curves may be ignored for present purposes.

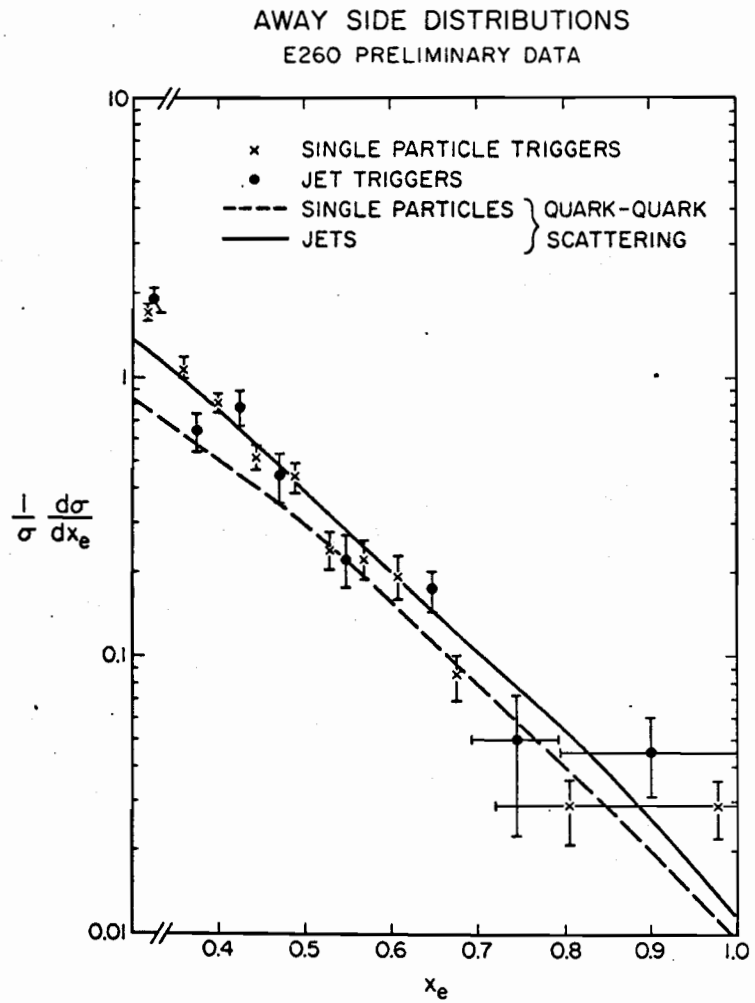

Fig. 7: Shows away side distribution is similar for jet and single particle distributions[30]. x_e for single particles is defined as .85 p_T (away particle)/ p_T (single particle trigger). No correction has been made for acceptance or background in data. The theory has been divided by 2 as an approximation to acceptance correction.

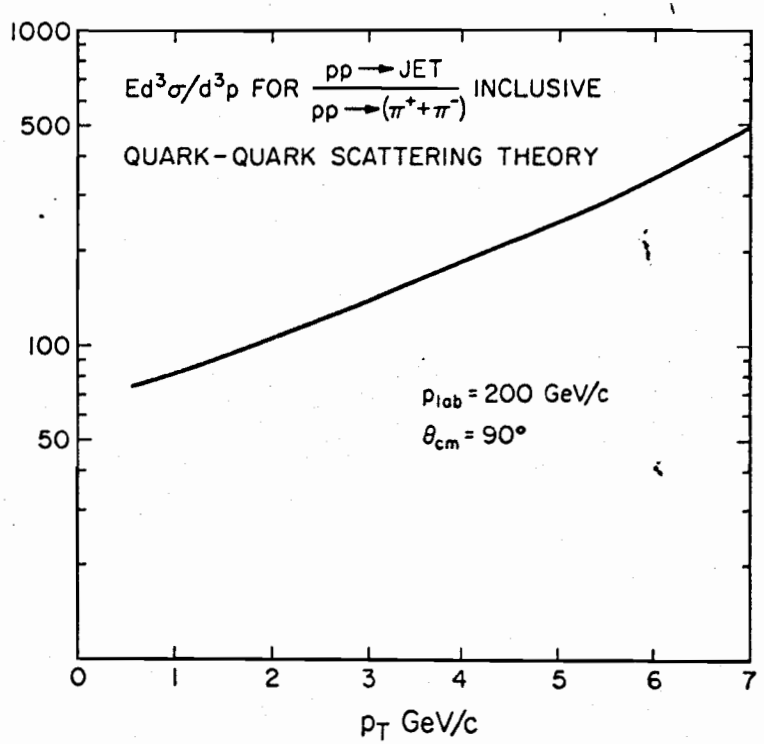

Fig. 8: Ratio of jet to single particle cross-sections in the Field Feynman quark-quark scattering model. The ratio is only a function of x_T in the theory and so this curve can easily be scaled to other incident momenta.

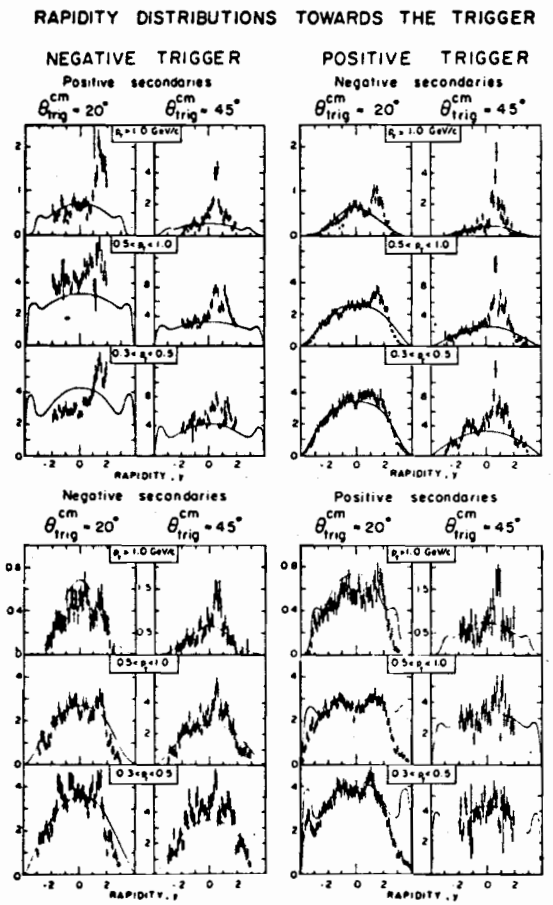

Fig. 9: Towards rapidity distributions from the CCHK collaboration[31]. Triggers are ± charges at θ=20° and 45° (rapidities 1.8 and .85) while secondaries have $|\phi| \leq 25^\circ$ with respect to trigger. The plotted quantity is $\frac{100}{\sigma}\ d\sigma/dy d\phi$. The solid lines represent minimum bias distributions.

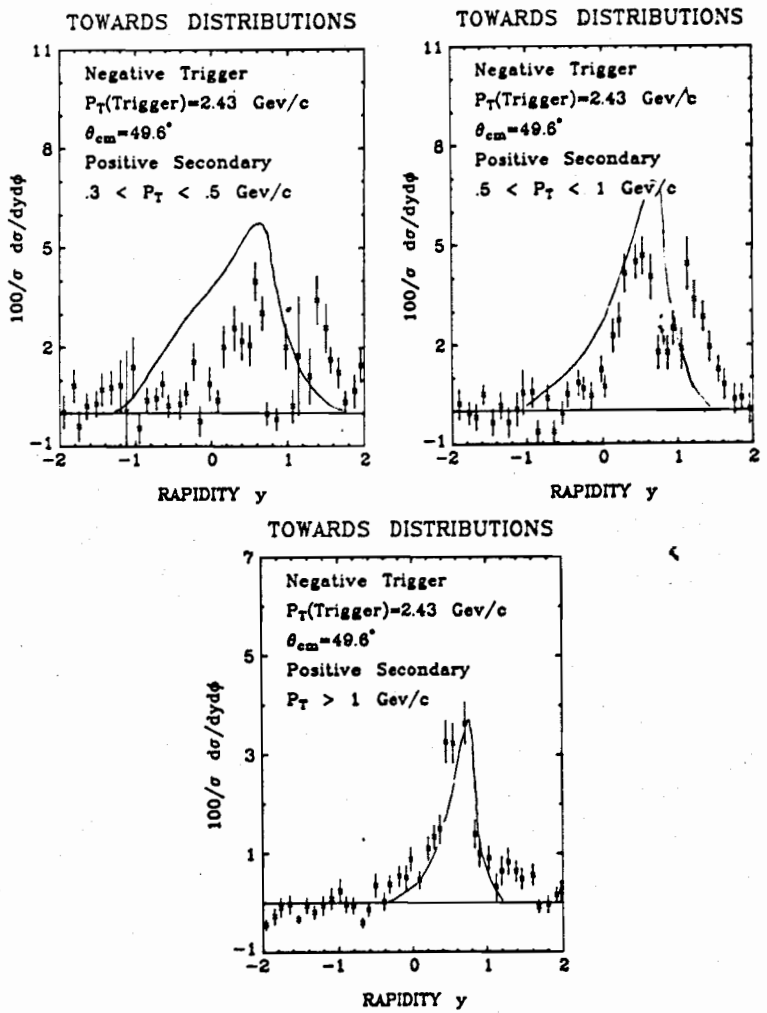

Fig 10: Comparison of 3 of the graphs, corresponding to - trigger and + secondary at 45°, shown in Fig. 9 from the CCHK collaboration[31], with the predictions of model Q. In this figure, we have done a simple subtraction of data points and background shown in Fig. 9.

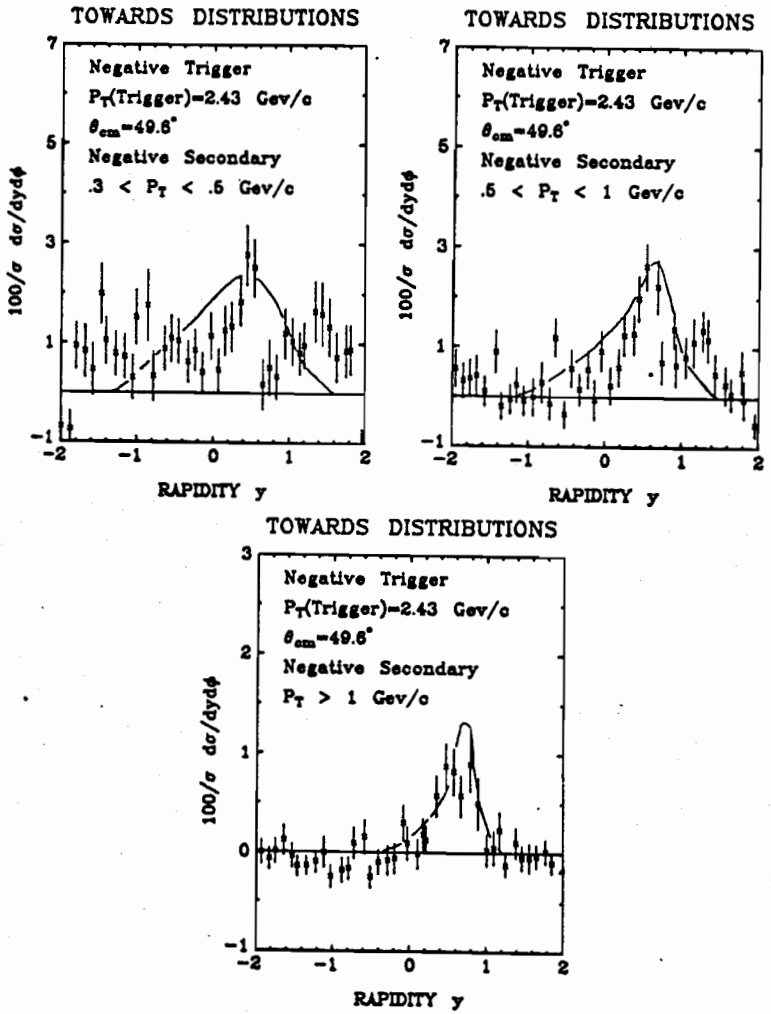

Fig. 11: Comparison of 3 of the graphs, corresponding to - trigger and - secondary at 45°, shown in Fig. 9 from the CCHK collaboration[31], with the predictions of model Q. In this figure we have done a simple subtraction of data points and background shown in Fig. 9.

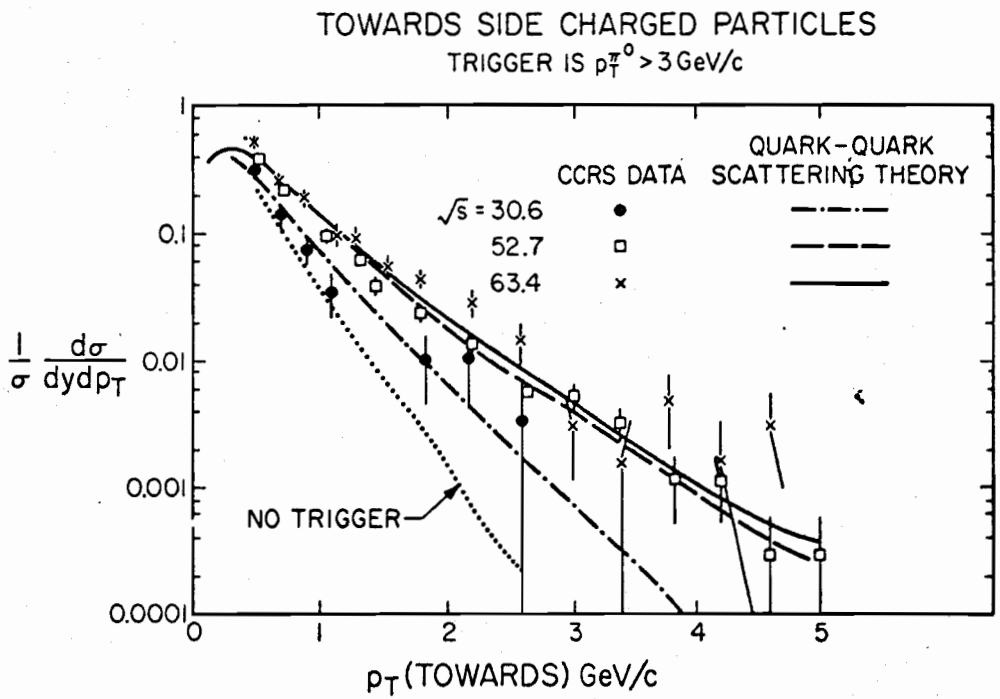

Fig. 12: Compares the energy dependence of the towards correlation function in the CCRS data[29] and the model Q theory. Please consult the original reference for definition of plotted quantity. Background (marked "no trigger") has not been subtracted from the data. Also one energy has been removed from plot for clarity.

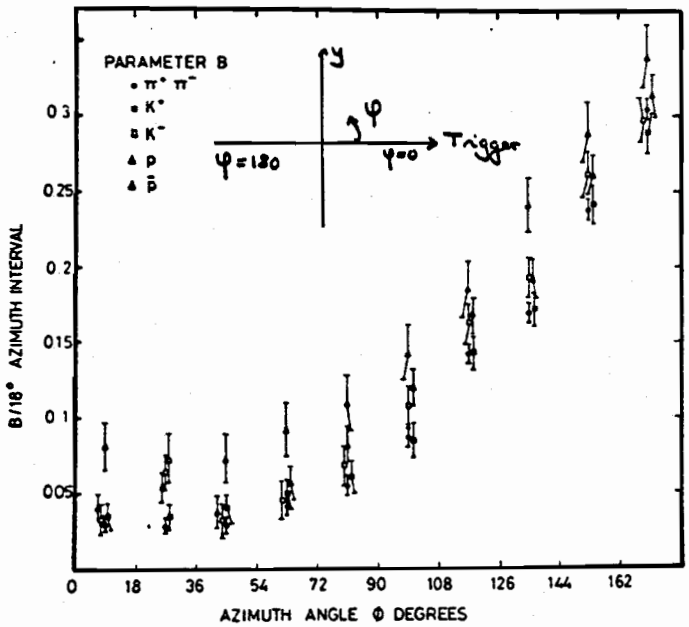

Fig. 13: Data from the DILR collaboration[36] shows the variation with ϕ and trigger particle type of the coefficient B of p_T for the expression in Eq. (4) of the associated multiplicity.

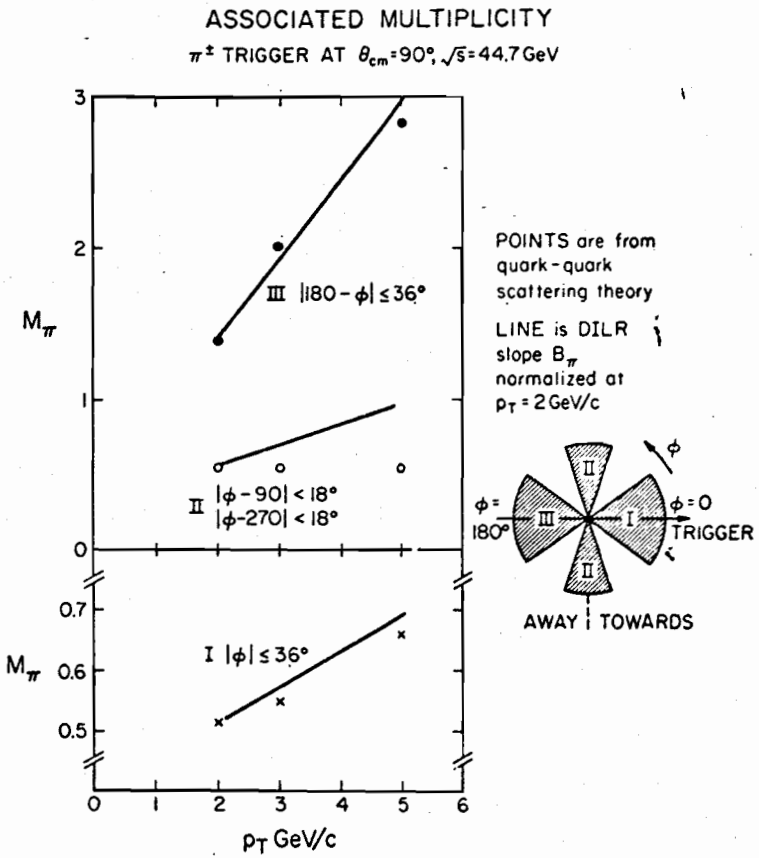

Fig. 14: Compares the quark quark scattering theory (model Q with $\exp(-6k_T)$ internal transverse momentum smearing) with a selection of DILR data[36] from the previous figure.

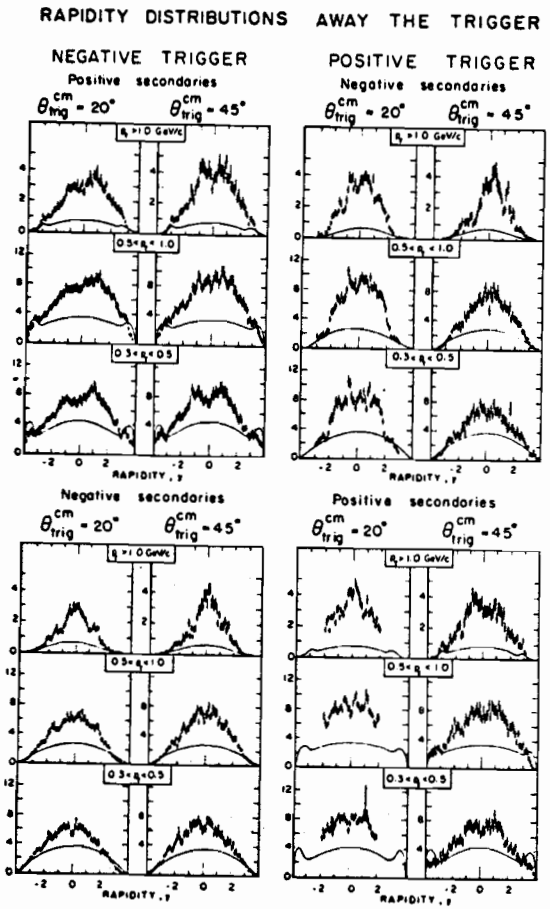

Fig 15: Away side rapidity distribution from the CCHK collaboration[31]. Triggers are ± charges at θ= 20° and 45° (rapidities 1.8 and .85) while secondaries satisfy $|180-\phi| \leq 40°$. The plotted quantity is $\frac{100}{\sigma} d\sigma/d\phi dy$. The solid lines represent minimum bias distributions.

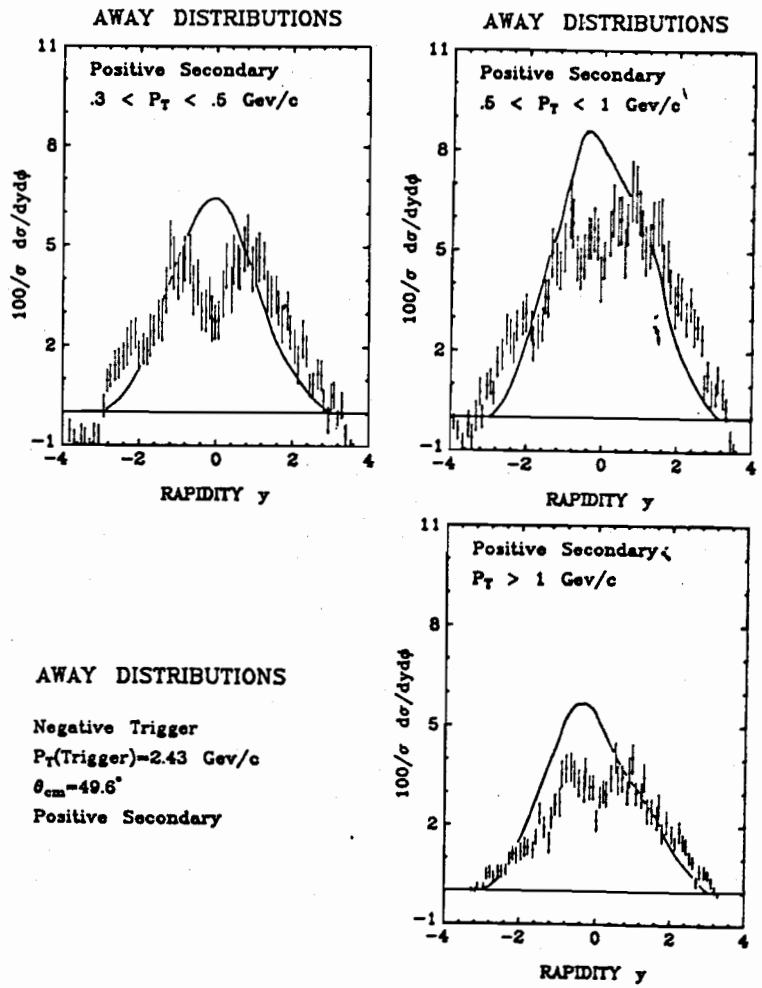

Fig. 16: Comparison of 3 of the graphs, corresponding to - trigger and + secondary at 45°, shown in Fig. 15 from the CCHK collaboration[31], with the predictions of model Q. The data represents a simple subtraction of signal and background in Fig. 15 while the theory used an $\exp(-6k_T)$ internal momentum smearing for the quarks.

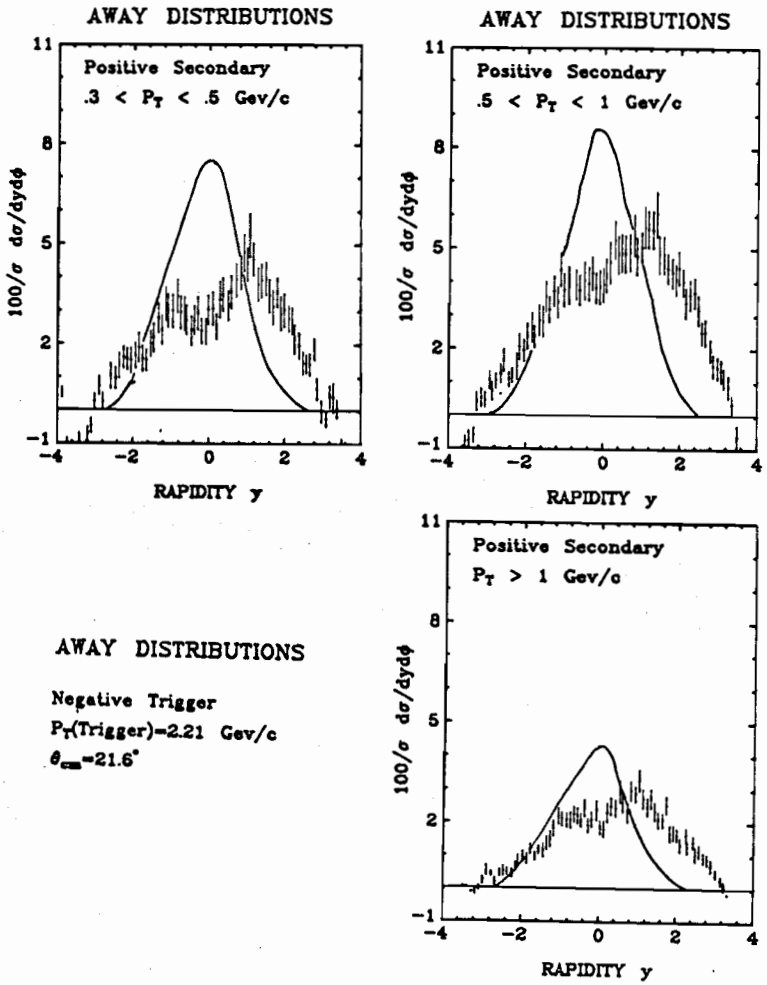

Fig. 17: Comparison of 3 of the graphs, corresponding to - trigger and + secondary at 20°, shown in Fig. 15 from CCHK collaboration[31], with the predictions of model Q. The data represents a simple subtraction of signal and background in Fig. 15 while the theory used an $\exp(-6k_T)$ internal momentum smearing for the quarks.

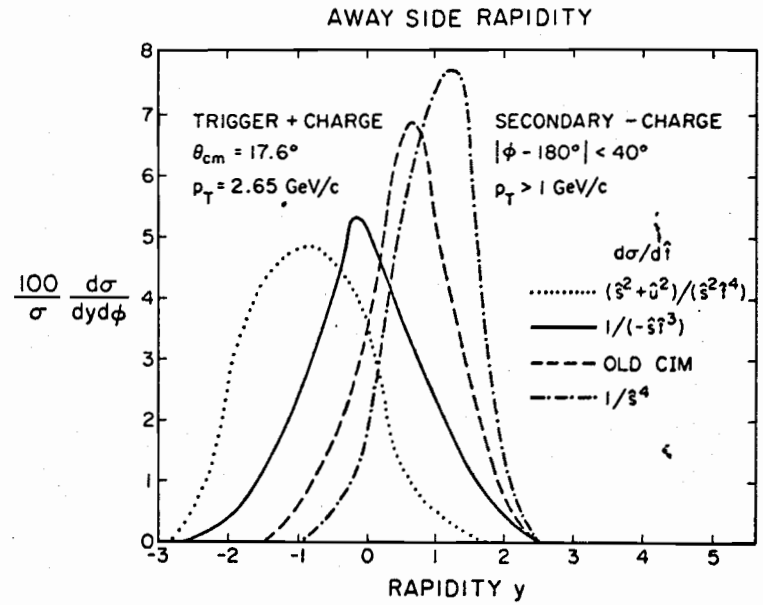

Fig. 18: Shows the variation of the away side rapidity distribution with the form of $d\sigma/d\hat{t}$ given in equations (5) and (6) of the text. All models used $\exp(-6k_T)$ internal transverse momentum smearing. The solid line gives the Field Feynman model which as shown in figures 16 and 17 has the same shape as the data. The curve marked "OLD CIM" uses the spin 0 quark equation (6): the more reasonable spin 1/2 model discussed in text is similar to solid line in figure.

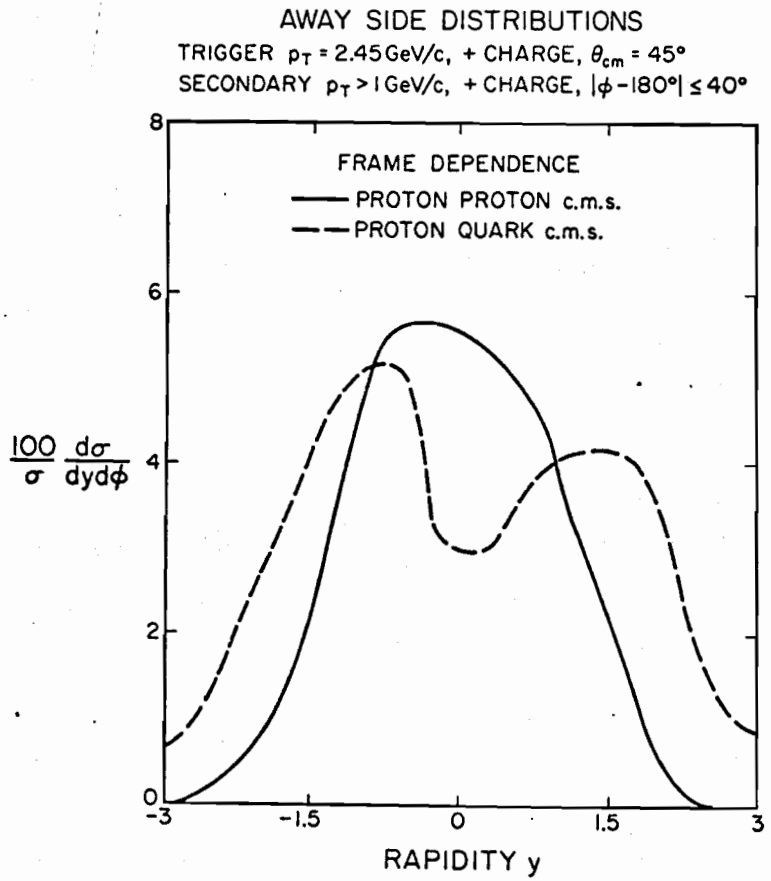

Fig. 19: Shows the frame dependence of the away side rapidity distributions. Both curves come from quark quark scattering with $\exp(-6k_T)$ internal transverse momentum smearing. The solid curve is the normal calculation. The dashed line lets quark d decay in extreme proton quark frame discussed in Section VII.

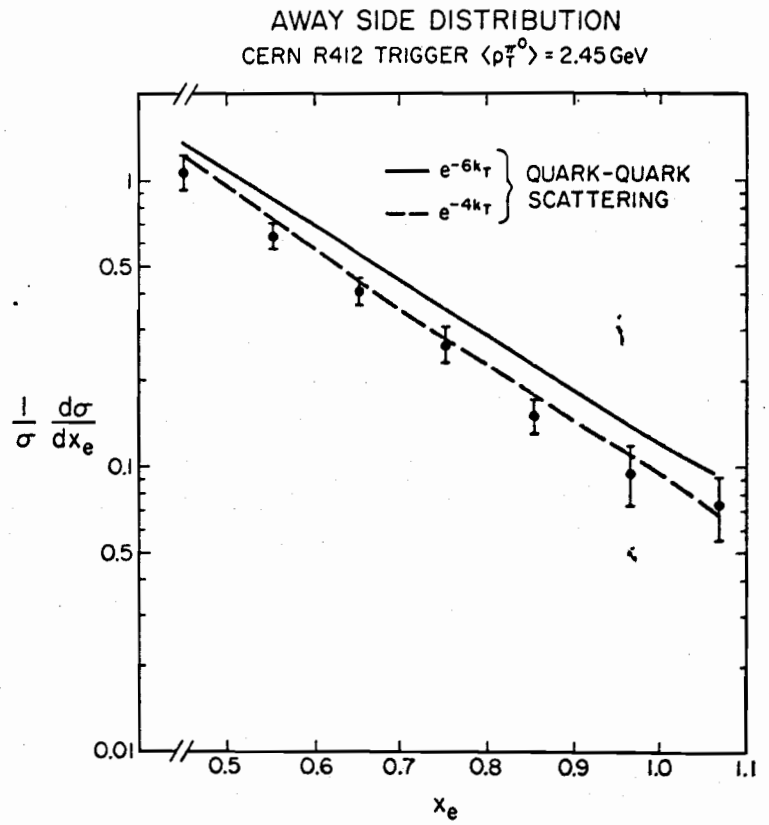

Fig. 20: Comparison of CERN R412[22] x_e distributions with quark quark elastic scattering. Two choices ($< k_T > = 330$, $< k_T > = 500$ MeV) are shown for internal transverse momentum smearing.

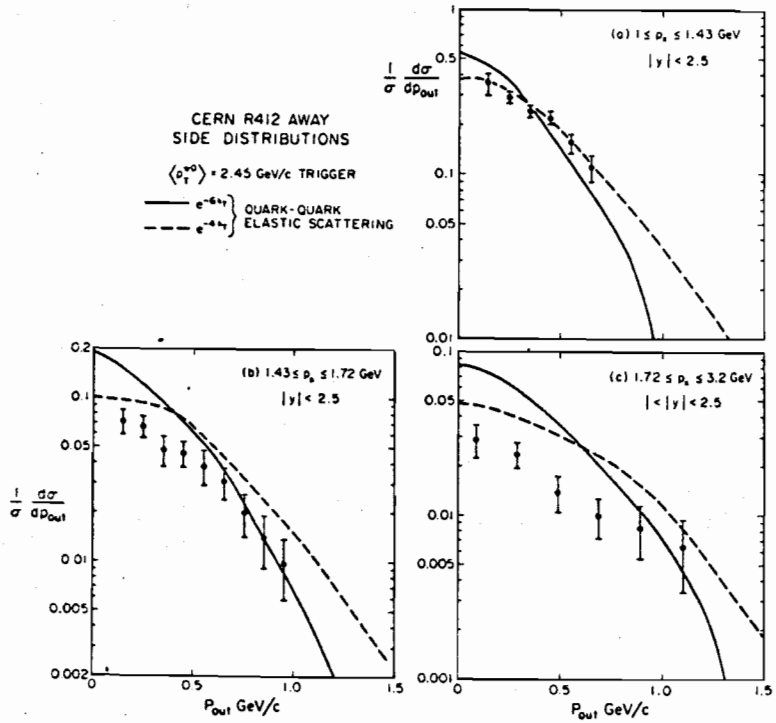

Fig. 21: Comparison of CERN R412[22] P_{out} distributions with quark quark elastic scattering. Two choices ($< k_T > = 330$, $< k_T > = 500$ MeV) are shown for internal transverse momentum smearing. The normalization of the theory is better studied in figure 20. Thus the overall size of theory for figure 21 is sensitive to p_T spectrum of trigger π^0's but figure 20 avoids this problem as x_e distributions scale (in theory).

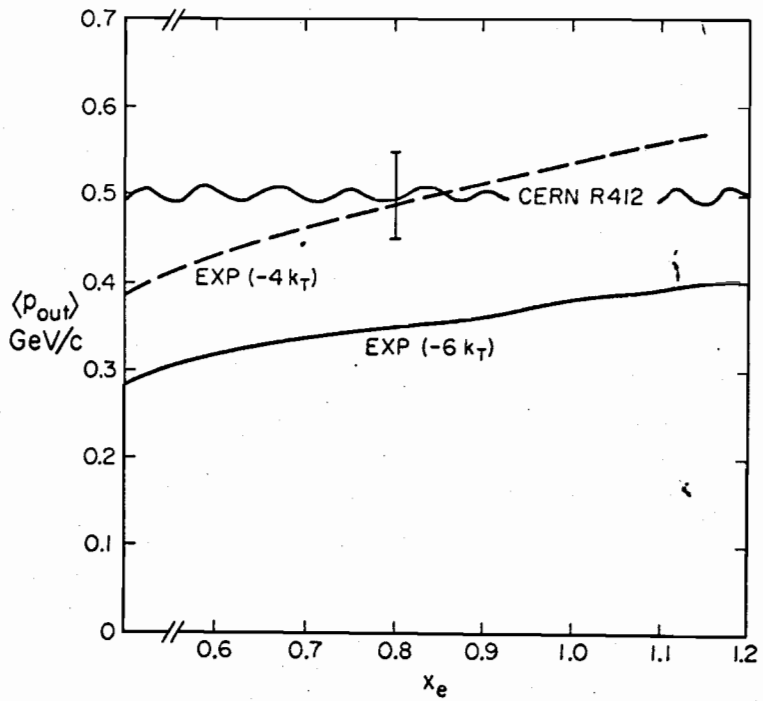

Fig. 22: Predicted x_e dependence of $< p_{out} >$ for $< k_T > = 330$, 500 internal transverse momentum smearing in quark quark elastic scattering model. Also shown is the CERN R412[22] experimental value of 0.5 ± .05 : within errors they see no x_e dependence.

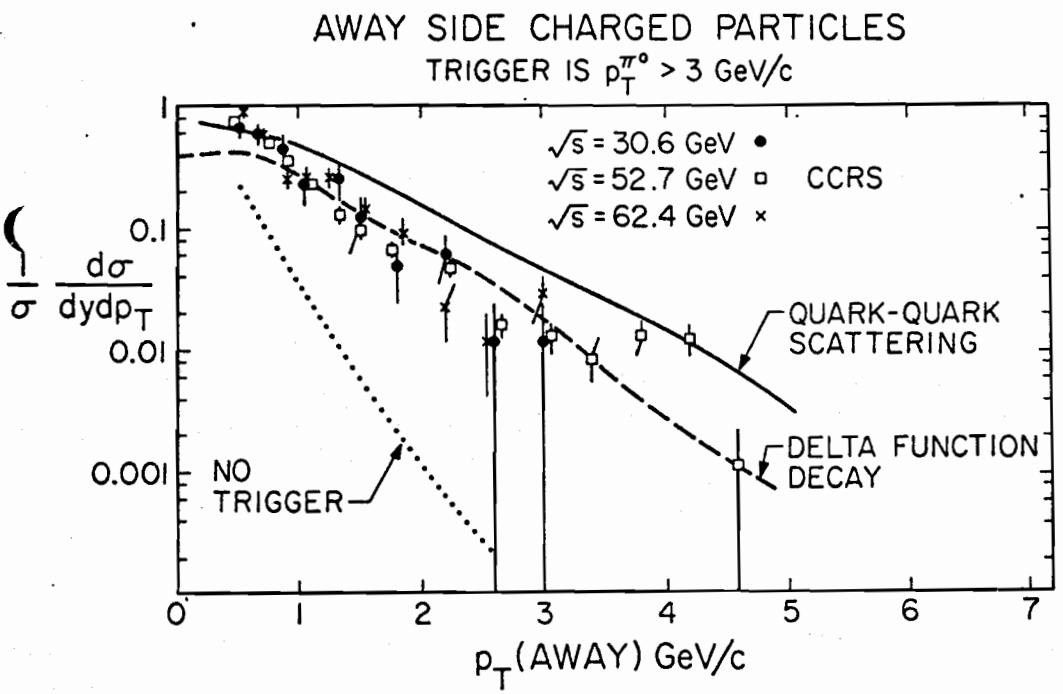

Fig. 23: Shows the away side distribution of charged particles for a π^0 trigger averaged over $p_T > 3$ GeV/C. The data comes from the CCRS collaboration[29] and their paper should be consulted for an exact definition of plotted quantity. The theory shows normal quark quark scattering (too big!) and the effect of using a delta function decay (model D). Background (marked "no trigger") has not been subtracted from the data. Also one energy has been removed from the plot for clarity. Both theory curves are essentially independent of incident energy.

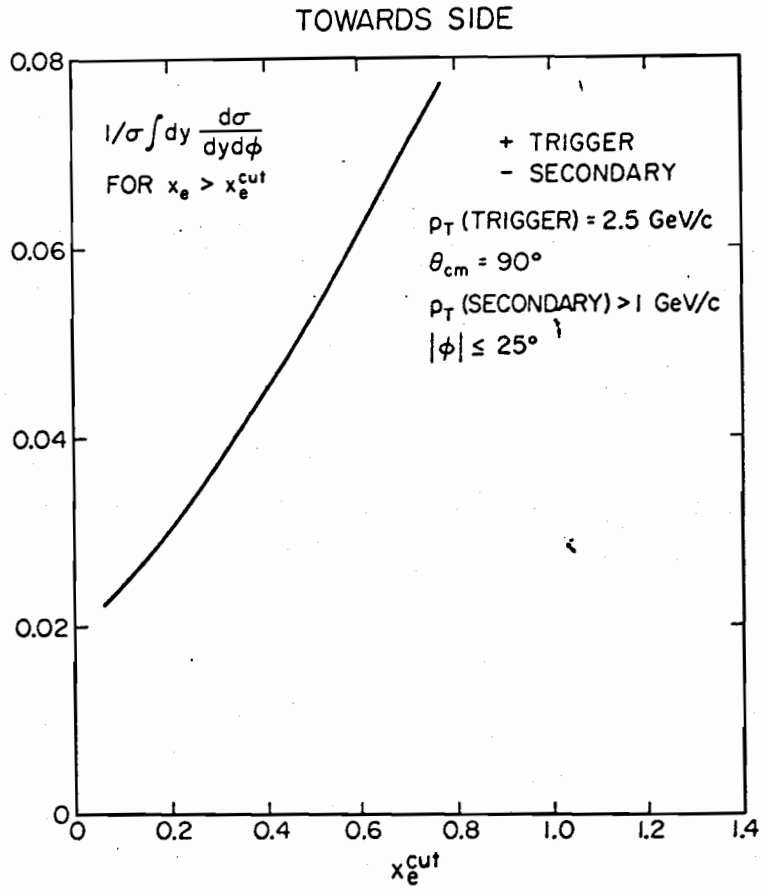

Fig. 24: (Jacob-Landshoff[33] effect) shows number of "towards" tracks per event with $p_T > 1$ GeV/c, $|\phi| \leq 25°$, when you also require a particle on the other side with $x_e \geq x_e^{cut}$. The theory is simple quark-quark elastic scattering.

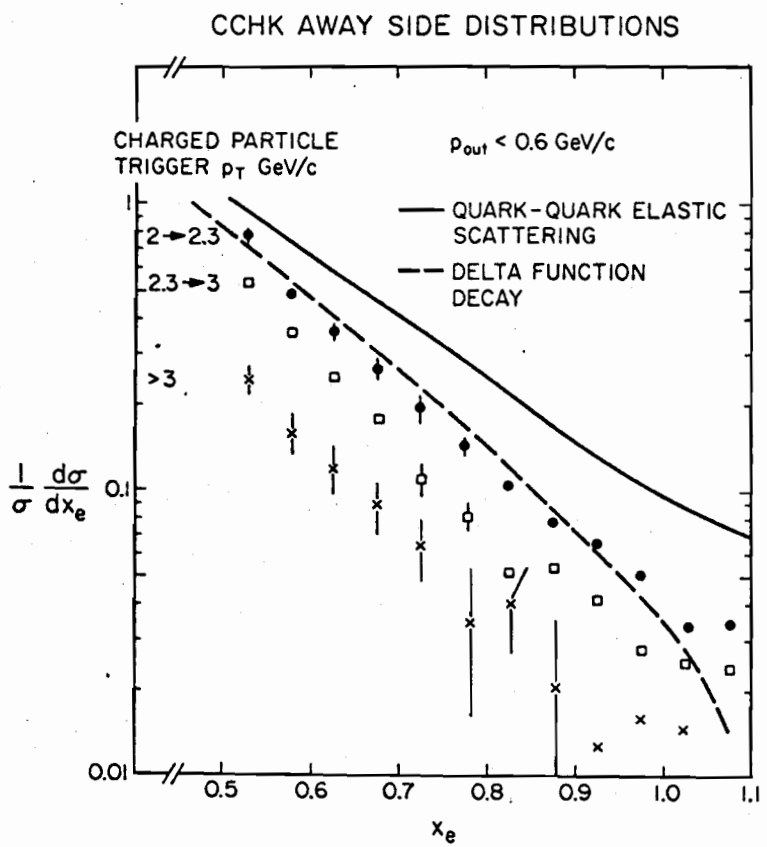

Fig. 25: (Total disaster) shows variation of $d\sigma/dx_e$ with trigger p_T from CCHK collaboration[4]. Shown are the p_T independent theoretical curves from both quark quark elastic scattering and the delta function decay model. Both used $\exp(-6k_T)$ internal transverse momentum